Local biodiversity change reflects interactions among changing abundance, evenness and richness

Shane A. Blowes, German Centre for Integrative Biodiversity Research (iDiv) Halle-Jena-Leipzig, Germany; Department of Computer Science, Martin Luther University Halle-Wittenberg, Halle (Salle), Germany. shane.blowes@idiv.de

Gergana N. Daskalova, School of GeoSciences, University of Edinburgh, Scotland EH9 3FF. gndaskalova@gmail.com

Maria Dornelas, Centre for Biological Diversity, University of St Andrews, KY16 9TH. maadd@st-andrews.ac.uk

Thore Engel, German Centre for Integrative Biodiversity Research (iDiv) Halle-Jena-Leipzig, Germany; Department of Computer Science, Martin Luther University Halle-Wittenberg, Halle (Salle), Germany. thore.engel@idiv.de

Nicholas J. Gotelli, Department of Biology, University of Vermont, Burlington, VT 05405 USA. Nicholas.Gotelli@uvm.edu

Anne E. Magurran, Centre for Biological Diversity, University of St Andrews, KY16 9TH. aem1@st-andrews.ac.uk

Inês S. Martins, Leverhulme Centre for Anthropocene Biodiversity and Department of Biology, University of York, York YO10 5DD, UK; Centre for Biological Diversity, University of St Andrews, KY16 9TH. iism1@st-andrews.ac.uk

Brian McGill, School of Biology and Ecology and Mitchell Center for Sustainability Solutions, University of Maine; Orono, ME. mail@brianmcgill.org

Daniel J. McGlinn, Department of Biology, College of Charleston, Charleston, SC. danmcglinn@gmail.com

Alban Sagouis, German Centre for Integrative Biodiversity Research (iDiv) Halle-Jena-Leipzig, Germany; Department of Computer Science, Martin Luther University Halle-Wittenberg, Halle (Salle), Germany. alban.sagouis@idiv.de

Hideyasu Shimadzu, Department of Mathematical Sciences, Loughborough University, LE11 3TU, UK; Graduate School of Public Health, Teikyo University, Tokyo, Japan. H.Shimadzu@lboro.ac.uk

Sarah R. Supp, Data Analytics Program, Denison University, Granville, OH 43023 USA. supps@denison.edu

Jonathan M. Chase, German Centre for Integrative Biodiversity Research (iDiv) Halle-Jena-Leipzig, Germany; Department of Computer Science, Martin Luther University Halle-Wittenberg, Halle (Salle), Germany. jonathan.chase@idiv.de

Running title: Characterizing multicomponent diversity change

Corresponding author: Shane Blowes, German Centre for Integrative Biodiversity Research (iDiv) Halle-Jena-Leipzig, Deutscher Platz 5e, Leipzig 04103, Germany. shane.blowes@idiv.de + 49 341 9733254.

Open research statement: All data used in the manuscript are already in the public domain. The BioTIME database is accessible through the BioTIME website (http://biotime.st-andrews.ac.uk) and a Zenodo repository (https://zenodo.org/record/1095627). Perturbed time series were compiled using the data portal of the Environmental Data Initiative (https://portal.edirepository.org/nis/home.jsp), query as described in the methods; code for compilation and standardization available at https://github.com/chase-lab/BioTIMEx; upon acceptance, this code will be stored in combination with the code for analyses (see below) in Zenodo. The 2016 release of the PREDICTS database as used here is available at https://data.nhm.ac.uk/dataset/the-2016-release-of-the-predicts-database. McGill SAD data were previously archived at: https://doi.org/10.6084/m9.figshare.6945704. CESTES database is available at https://doi.org/10.25829/idiv.286-21-2695. Code for all analyses is available at https://github.com/sablowes/MulticomponentBioChange; upon acceptance, this code will be stored (with code for accessing and cleaning the EDI data described above) in Zenodo.

Abstract

Biodiversity metrics often integrate data on the presence and abundance of multiple species. Yet understanding covariation of changes to the numbers of individuals, the evenness of species' relative abundances, and the total number of species remains limited. Using individual-based rarefaction curves, we introduce a conceptual framework to understand how expected positive relationships among changes in abundance, evenness and richness arise, and how they can break down. We then examined interdependencies between changes in abundance, evenness and richness in more than 1100 assemblages sampled either through time or across space. As predicted, richness changes were greatest when abundance and evenness changed in the same direction, and countervailing changes in abundance and evenness acted to constrain the magnitude of changes in species richness. Site-to-site changes in abundance, evenness, and richness were often decoupled, and pairwise relationships between changes in these components across assemblages were weak. In contrast, changes in species richness and relative abundance were strongly correlated for assemblages varying through time. Temporal changes in local biodiversity showed greater inertia and stronger relationships between the component changes when compared to site-to-site variation. Local variation in assemblage diversity was rarely due to a passive sample from a more or less static species abundance distribution. Instead, changing species relative abundances often dominated local variation in diversity. Moreover, how changing relative abundances combined with changes to total abundance frequently determined the magnitude of richness changes. Embracing the interdependencies between changing abundance, evenness and richness can provide new information for better understanding biodiversity change in the Anthropocene.

Keywords: biodiversity change, abundance, evenness, species richness, rarefaction

Introduction

Measures of biodiversity and its change are frequently used to determine the magnitude, direction and pace of ecosystem modifications (Diaz et al. 2019). Descriptions of the distribution and abundance of organisms are central to basic ecological research (Krebs 1972, Andrewartha & Birch 1984), and biodiversity (as applied to taxonomic or species diversity) is a multifaceted concept that combines information on the distribution and abundance of multiple species. There have been numerous such aggregate metrics proposed to quantify different aspects of biodiversity (e.g., Hill 1973, Gotelli and Colwell 2001, Magurran & McGill 2011, Chao and Jost 2012), most of which depend on sample effort and scale (Rosenzweig 1995, Whittaker et al. 2001, McGill 2011a, Chase & Knight 2013). This inherent complexity poses significant challenges for quantitative syntheses of temporal and spatial variation in biodiversity.

Here, we argue that in order to understand biodiversity change, it is critical to look beyond aggregate metrics in isolation. Specifically, we need to examine how changes in the key components that lead to aggregate metrics interact and combine with each other. Currently, different components that underlie biodiversity represent important, but are largely viewed as independent lines of evidence for contemporary biodiversity change. For example, one body of work is focused on quantifying total abundances of all species within assemblages, such as recent work documenting declines of birds (e.g., Rosenberg et al. 2019) and insects (Wagner 2020). A related body of work focuses instead on population-level ‘winners’ and ‘losers’ within assemblages (McKinney & Lockwood 2000), species with increasing and decreasing trends in occupancy or abundance (e.g., WWF 2020). However, changes in the means of these metrics do not capture the variability and nuance in either the assemblage- and population-level abundance

112 trends across space and among taxa (e.g., van Klink et al. 2020, Daskalova et al. 2020a, Leung et
113 al. 2020). Moreover, trends in total assemblage abundance provide only one window into
114 potentially complex changes that could be occurring in other components of biodiversity, and
115 while changes to species relative abundances do influence biodiversity metrics, population-level
116 trends themselves cannot be used to calculate assemblage-level (i.e., biodiversity) metrics (e.g.,
117 Dornelas et al. 2019). Even when quantifying the same response metric (i.e., species richness),
118 syntheses of biodiversity change in space due to differential land use conditions have found
119 declines of species richness (e.g., Newbold et al. 2015, 2018), whereas analyses of time series
120 have shown that, on average, species richness increases roughly offset decreases (Dornelas et al.
121 2014, Blowes et al. 2019), despite often significant modifications to climate and habitat (Antão
122 et al. 2020a, Daskalova et al. 2020b). Finally, the prediction that human activities likely impact
123 species relative abundances more frequently than species occurrences (Chapin et al. 2000), has
124 not resulted in a strong focus on assemblage-level evenness in existing syntheses (but see, e.g.,
125 Crowder et al. 2010, Zhang et al. 2012, Jones & Magurran 2018). Importantly, changes in all
126 these components -- abundance, evenness, and richness -- contribute to variation in biodiversity.
127 Yet little is known about how components are changing in combination within assemblages, and
128 whether certain combinations act to constrain observed biodiversity change.
129
130 Species origination (speciation plus colonization) and extinction are the most fundamental
131 processes for biodiversity dynamics (Storch et al. 2021). These processes combine with
132 productivity (Currie 1991, Mittelbach et al. 2001), disturbance frequency and intensity (Connell
133 1978, Miller et al. 2011), historical (Latham & Ricklefs 1993) and biogeographic factors (e.g.,
134 Kreft et al. 2008), land use modifications (Newbold et al. 2015), and climate change (Antão et al.

2020a) to drive variation in biodiversity. In turn, these processes and drivers combine such that local scale measures of biodiversity estimated from a given (local) sample depends largely on two components (see e.g., He and Legendre 2002, McGill 2011a). First, the total number of individuals (Fisher et al. 1943, Preston 1962), whereby fewer individuals are expected to (non-linearly) lead to fewer species. Second, the total number of species and their relative abundances within the regional species pool (i.e., the set of all potential colonizing species in a region), which we refer to as the Species Abundance Distribution (SAD; McGill et al. 2007). Local samples will have lower species richness when the species pool has relatively few highly abundant species and many rare species (i.e., less even SADs), compared to samples from a species pool of the equivalent size with more equitable species abundances. Moreover, variation or changes in local environmental conditions can alter local patterns of species relative abundances. Whenever two or more samples across space or time differ in the total number of individuals, the shape of the SAD, or both, there will be changes in most metrics of biodiversity. However, changes in abundance and the SAD are not always correlated, and, when decoupled, the magnitude and direction of change in derived biodiversity metrics can differ considerably.

Variation in the total number of individuals is a long-standing, first-order explanation of variation in richness (Fisher et al. 1943, Coleman et al. 1982, Srivastava & Lawton 1998, Gaston 2000, Scheiner & Willig 2005, Storch et al. 2018). In the context of species-area relationships, this has been termed the ‘passive sampling hypothesis’ (Coleman et al. 1982), and as local assemblages increase in size they are expected to include more species from the regional pool due to sampling processes alone. Larger (Connor & McCoy 1979) or more productive (Wright 1983) areas are also predicted to have more species driven again by increased numbers of

158 individuals, but in these cases associated with processes other than sampling, such as decreased
159 likelihood of species extinction with increased population sizes (Preston 1962, Wright 1983,
160 Srivastava & Lawton 1998), and commonly termed the 'more individuals hypothesis' (Srivastava
161 & Lawton 1998). Anthropogenic drivers can also influence the number of individuals in
162 assemblages (e.g., via eutrophication, exploitation, harvesting or land clearing), potentially
163 impacting biodiversity due to changes to the total number of individuals (Newbold et al. 2015,
164 Blowes et al. 2020). If biodiversity varies primarily via changes in the numbers of individuals,
165 positive relationships between altered numbers of individuals and species richness changes are
166 expected. In such cases, however, other metrics of species diversity that control for variation in
167 numbers of individuals, such as species richness expected for a given number of individuals—
168 known as rarefied richness—should be relatively unchanged.
169
170 Changes to the shape of the SAD can drive variation in biodiversity through time or space. For
171 example, co-occurrence and coexistence of species can be altered by changes to resource
172 diversity (MacArthur 1965), environmental or habitat heterogeneity (Tilman 1982, Shmida &
173 Wilson 1985), interspecific interactions (e.g., keystone predation; Paine 1974, Menge et al.
174 2020), biological invasions (Vilà et al. 2011), and external perturbations (Hughes et al. 2007).
175 Alterations to any of these features can change biodiversity by changing species' relative
176 abundances and the size of the species pool (via species additions or subtractions).
177 Anthropogenic factors can also favor some species and disfavor others, potentially altering the
178 relative abundance of species (e.g., due to selective exploitation; Blowes et al. 2020), or the size
179 of the species pool (e.g., species with large ranges replacing those with small ranges, Newbold et
180 al. 2018). In such cases, biodiversity change will be characterized by positive relationships

between species richness change and changes in metrics sensitive to relative abundance, such as rarefied richness, evenness and diversity metrics sensitive to species relative abundances.

Changing components of biodiversity can covary in different and informative ways. Yet, to date, there has been little exploration of this covariation in time or space, nor of the theoretical linkages. For example, whether total abundances and the evenness of species' relative abundances change in similar or decoupled ways, and how this influences biodiversity change is largely unknown. However, syntheses of relationships between different biodiversity metrics, which can reflect different combinations of component changes, have typically found relationships to be weak. For example, Stirling and Wilsey (2001) showed that although strong positive correlations between species richness, diversity and evenness metrics were expected from a neutral model (Caswell 1976), there was considerable variation in the strength, and even the sign of the relationships in 323 empirical comparisons. Similarly, Soininen et al. (2012) examined temporal (n = 212) and spatial variation (n = 17) in aquatic datasets, and again found considerable heterogeneity in the relationship between richness and evenness. Using data from 91 assemblages, McGill (2011b) concluded that most biodiversity metrics align with three axes of empirical variation (total abundance, evenness and richness); components subsequently shown to be relatively uncorrelated across space for a subset of 37 of the 91 assemblages (Chase et al. 2018). Collectively, these studies suggest that static biodiversity estimates are multidimensional, and that different metrics can covary or be unrelated.

Where ecologists have quantified variation in multiple components of local diversity, the focus has typically been on averages across assemblages, with each component treated as a separate,

204 independent response. For example, analyses of the local assemblages documented by the
205 BioTIME database (Dornelas et al. 2018) show that numbers of individuals, species richness, and
206 dominance (quantified as the relative abundance of the most numerically dominant species, and
207 conceptually the complement of evenness) are highly variable among datasets, but on average,
208 have no directional trend (Dornelas et al. 2014, Jones & Magurran 2018, Blowes et al. 2019). On
209 the other hand, analyses of the PREDICTS database (Hudson et al. 2017) documenting spatial
210 contrasts between assemblages in more pristine habitats with those in different land use
211 categories, show that human-altered habitats frequently have fewer species and often fewer
212 individuals (Newbold et al. 2015, 2020). However, these results describe average changes across
213 assemblages estimated independently, whereas, as we describe in more detail below, component
214 changes are unlikely to be completely independent.
215
216 Here, we first provide a conceptual overview of how changes in the main components underlying
217 local biodiversity (total abundance, evenness and species richness) can combine using
218 individual-based rarefaction curves. Using simplified scenarios with contrasting component
219 changes, we show that the signs (or direction) of changes in total abundance and evenness can
220 combine to determine the magnitude of expected richness changes, and whether positive
221 pairwise relationships prevail. We then empirically assess interdependencies between abundance,
222 evenness and richness changes using compilations of ecological assemblage data. In the face of
223 natural and anthropogenically-driven environmental variation in time and space, we ask whether
224 changes in the components of local biodiversity show positive relationships (i.e., change in the
225 same direction). Or, alternatively, are component changes sufficiently heterogeneous that

variation in biodiversity depends on which of the underlying components (numbers of individuals or the SAD) are changing, and how the different component changes combine?

Conceptual relationships between changes in total abundance, evenness and richness

Individual-Based Rarefaction (IBR) curves (Hurlbert 1971, Gotelli & Colwell 2001) are well suited for visualizing conceptual relationships among changes in total abundance, evenness and species richness (Fig. 1a, Cayuela et al. 2015, Chase et al. 2018, McGlinn et al. 2019). The end point of the IBR depicts the total number of individuals of all species combined, and variation between assemblages in where the IBR terminates quantifies changes to the number of individuals (ΔN, Fig.1a) and species richness (ΔS, Fig. 1a). The shape (or curvature) of the IBR curve reflects species' relative abundances and the size of the species pool (i.e., the SAD). We use two parts of the curve to characterize changes in the SAD between assemblages. First, because it is standardized to an equal number of individuals (n), changes in rarefied richness, ΔS_n (Fig.1a), reflects changes to species' relative abundances only. Second, we use the numbers equivalent (or effective number of species) transformation of the Probability of Interspecific Encounter (PIE, Hurlbert 1971). The PIE is equal to the slope at the base of the rarefaction curve (Olszewski 2004) and represents a metric of evenness that is relatively insensitive to sample effort (more even communities have a higher PIE, Fig. 1a). Transformation of the PIE to the numbers equivalent (S_{PIE}) aids comparisons to species richness (i.e., ΔS and ΔS_{PIE} have the same units; Jost 2006). S_{PIE} is equal to the inverse of Simpson concentration (Jost 2006), and diversity of order $q = 2$ (Hill 1973, Jost 2007), $D = (\sum_{i=1}^{S} p_i^q)^{1/(1-q)} = \frac{1}{\sum_{i=1}^{S} p_i^2}$, where S is the number of species and p_i is the proportion of the assemblage represented by species i. As a consequence,

248 changes in S_{PIE} (ΔS_{PIE}) are most strongly influenced by the number of abundant or common
249 species in assemblages.
250
251 To visualize relationships among changes in total abundance, evenness and richness, we plot
252 pairwise relationships between changes in four components of the IBR. Specifically, changes in
253 species richness (ΔS) and total abundance (ΔN; Fig. 1b), and species richness and the two metrics
254 sensitive to changes in relative abundance – rarefied richness, ΔS_n (Fig. 1c), and ΔS_{PIE}, which we
255 refer to as evenness (Fig. 1d). Changing components with positive relationships (i.e., the same
256 sign) fall into the lower left and upper right quadrants, whereas assemblage changes that fall into
257 the upper left or lower right quadrants of Figs. 1b, c, d reflect a negative relationship between the
258 respective components.
259
260 Altered numbers of individuals, but no change to the SAD, can underpin differences in diversity
261 between assemblages. Changes only to the number of individuals being passively sampled from
262 the same underlying SAD (Fig. 2a) result in ΔS and ΔN being positively related with the same
263 sign (Fig. 2g), whereas ΔS_n (Fig. 2h) and ΔS_{PIE} (Figs. 2i) will be approximately zero (and have a
264 weak or no relationship with ΔS). This has been variously referred to in the literature as a
265 sampling effect, the rarefaction effect, and the passive sampling hypothesis (Coleman et al. 1982,
266 Gotelli & Cowell 2001, Palmer et al. 2000).
267
268 Changes in species richness (ΔS) can also be solely associated with changes to relative
269 abundance (i.e., $\Delta N \approx 0$), which weakens or removes the expectation for a positive relationship
270 between changes in richness and total abundance. For example, changes in species richness can

271 be associated with SAD changes due, for e.g., to increased numbers of common species,
272 increased evenness (He & Legendre 2002), or increases to the size of the species pool (Fig. 2b),
273 which results in a positive relationship between ΔS and ΔS_{PIE} (Figure 2i). Finally, if total
274 abundance and relative abundance change in the same direction (e.g., more individuals and
275 increased evenness, Fig. 2c), then positive pairwise relationships are expected between changes
276 in abundance, evenness and richness (Figs. 2g, h, i).
277
278 In contrast, even if numbers of individuals increase ($\Delta N > 0$), expected gains in species richness
279 can be constrained by decreased evenness. For example, opposing changes in total abundance
280 and evenness can potentially result in no change to species richness (Fig. 2d), and no relationship
281 between ΔS and ΔN (Fig. 2g). Or, if changes to the SAD are sufficiently strong, they can offset
282 any expected gains due to more individuals (Fig. 2e), and result in a negative relationship
283 between ΔS and ΔN (Fig. 2g). Alternatively, opposing changes to total numbers of individuals
284 and evenness could result in a positive relationship between ΔS and ΔN if, for example, the
285 effects of more individuals on species richness outweighs that of decreased evenness (Figure 2f).
286
287 These simplified scenarios illustrate the potential for interdependencies between component
288 changes. In particular, they show that the signs of changes in total abundance and evenness (i.e.,
289 ΔN and ΔS_{PIE}) can strongly influence the magnitude of richness changes, and whether expected
290 positive relationships between changes in abundance, evenness and richness are found. ΔN is
291 associated with the IBR curve stretching or contracting along the x-axis, and ΔS_{PIE} characterizes
292 changes that flex the curve up or down from the base along the y-axis (Olszewski 2004). When
293 ΔN and ΔS_{PIE} have the same sign, assemblages are expected to fall into the lower left and upper

294 right quadrants of Figs. 2g-i (i.e., component changes with the same sign and positive pairwise
295 relationships). In contrast, when ΔN and ΔS_{PIE} have different signs, they can have countervailing
296 effects that constrain richness changes, the strength of their pairwise relationships with ΔS will
297 be diminished and potentially reversed, and the likelihood of assemblages falling into the upper
298 left and lower right quadrants of Figs. 2g-i increases (i.e., opposing signs and negative pairwise
299 relationships).
300
301 **Empirical relationships among total abundance, evenness and richness**
302 Next, we evaluate empirical relationships by fitting models that allow for correlations between
303 component changes to data from 1125 assemblages. Our goal for the empirical analyses was to
304 examine relationships between changing components in temporal and spatial contexts across a
305 broad range of environmental conditions. We compiled data documenting either temporal or
306 spatial variation of assemblage composition in one of either naturally-varying or perturbed
307 environmental conditions. Temporal variation quantified rates of change (i.e., per year) for each
308 component for an assemblage at a single location through time. Analyses of spatial variation
309 quantified component changes between sites in different land use categories in perturbed
310 environments, or between random pairs of sites in the naturally-varying environment.
311
312 Based on our conceptual overview, we expect pairwise relationships between abundance,
313 evenness and richness changes to be generally positive. Changes in species richness are also
314 expected to be largest for assemblages where all pairwise relationships are positive. In contrast,
315 opposing changes in total abundance and evenness (i.e., ΔN and ΔS_{PIE} have different signs) are
316 expected to constrain changes in species richness. Additionally, if local diversity changes are

dominated by altered total abundances and species richness, strong positive relationships between ΔS and ΔN, but weaker relationships between ΔS and ΔS_n, and ΔS and ΔS_{PIE} should emerge across assemblages. Alternatively, strong relationships between either ΔS and ΔS_n and/or ΔS and ΔS_{PIE}, accompanied by a weaker relationship between ΔS and ΔN, would indicate that changes to the SAD are the dominant component of local assemblage change.

Temporal comparisons: natural environmental variation

Temporal changes in natural assemblages at the local scale were quantified using the BioTIME database (Dornelas et al. 2018). Annual rates of change (change per year) for each metric were estimated with models fit to data that documents over 45 thousand species in time series with an average duration of 13 years. Taxonomic groups in our analysis came from surveys in marine, freshwater and terrestrial ecosystems, and included plants (and other producers), invertebrates, fish, amphibians, reptiles, birds, and mammals, as well as several surveys that collected data from multiple taxa. Here, we only used time series that had numerical abundance data available (i.e., studies that recorded counts of the number of individuals for each species in an assemblage), and our analysis included 288 studies. Locations sampled in the BioTIME database document places with varying degrees of anthropogenic environmental change, but do not include manipulated assemblages or before-after-control-impact studies (Dornelas et al. 2018). Accordingly, we contrast the environmental variation sampled by BioTIME with assemblage time series that experienced documented perturbations (see *Temporal comparisons: experimental or natural perturbations*).

339 To quantify changes at the local scale within BioTIME, studies with large extents were broken
340 up into smaller cell-level time series, while still maintaining the integrity of individual studies
341 (i.e., different studies were not combined, even when samples were collected in the same grid
342 cell). We used sample-based rarefaction (Gotelli & Colwell 2001) to standardize the number of
343 samples per year for each time series (see Blowes et al. 2019 for details). For the calculation of
344 rarefied richness (S_n), the minimum total number of individuals was determined for each time
345 series, and set as the target n for which expected richness was calculated; cell-level time series
346 where $n < 5$ were discarded. This process resulted in 42,604 cell-level time series from the 288
347 studies, and we focus on the study-level estimates of change in our results and discussion.
348
349 *Temporal comparisons: experimental or natural perturbations*
350 To complement the environmental variation sampled by the BioTIME database, we searched for
351 time series data with either experimental or natural perturbations. Specifically, we queried the
352 U.S. LTER network using the Data Portal of the Environmental Data Initiative
353 (https://portal.edirepository.org/nis/home.jsp) with the search terms 'experiment' and 'time' and
354 'abundance'. Records returned were checked to confirm that samples documented assemblages
355 of similar species collected with the same methodology, and following data standardization (i.e.,
356 minimum of five individuals per sample, and standardization of sample effort through time), our
357 analysis included 11 studies (see Appendix S1: *Temporal comparisons: experimental or natural*
358 *perturbations* for references), and annual rates of change (i.e., per year) were estimated for 63
359 study-treatment combinations; rates of change for all treatments (including controls) were
360 quantified in our analyses. Natural and experimental treatments included changes due to

361 warming, eutrophication, fire, grazing, restoration, severe storms or other disturbances, and kelp
362 removal. Taxonomic groups included algae, plants, invertebrates, fish, birds, and mammals.
363
364 *Spatial comparisons: natural environmental variation*
365 We combined two existing compilations of data to examine spatial patterns of biodiversity
366 change in relatively natural environmental contexts. The CESTES database (Jeliazkov et al.
367 2019) contains assemblage data from studies that sampled species at multiple sites (it also
368 includes information on traits and environment that we do not use here); we removed studies
369 with explicit human impacts identified as an environmental feature, and our analysis included 19
370 studies that sampled terrestrial, freshwater and marine assemblages from a number of taxonomic
371 groups (birds, plants, insects, macroinvertebrates, fishes and mammals). McGill (2011b)
372 compiled datasets with two or more local assemblages containing species abundance data; we
373 removed studies documenting disturbances and other perturbations, resulting in 32 studies being
374 retained. From the combined 51 studies, those with many sites were randomly subsampled down
375 to ten sites so that they did not dominate the results. Within each study, an arbitrary site was
376 assigned as the 'reference' site, and change was quantified between every site and the reference
377 within studies; our analysis included a total of 356 spatial comparisons.
378
379 *Spatial comparisons: anthropogenic perturbations*
380 To quantify spatial differences in biodiversity due to anthropogenic land use, we used the
381 PREDICTS database (Hudson et al. 2017). We used the 2016 release of the database
382 (downloaded from https://data.nhm.ac.uk/dataset/the-2016-release-of-the-predicts-database on
383 10th July 2020). We limited our analyses to studies with abundance data for individuals, and

384 those with known land use categories (primary vegetation, mature secondary vegetation,
385 intermediate secondary vegetation, plantation forest, cropland, pasture, and urban); studies where
386 land use was not recorded were omitted. This resulted in 237 combinations of source ID and
387 study (some sources had multiple studies, denoted SS in the database), and 418 estimates of
388 change relative to the reference land use (primary vegetation) category.
389
390 *Statistical models*
391 To estimate changes in the different metrics whilst accounting for expected correlations between
392 them, we fit multivariate multilevel models to the data. Similar to the way univariate multilevel
393 (also called hierarchical or mixed-effects) models fit to a single response can allow varying (also
394 called random) intercepts and slopes to be correlated, this approach estimates changes in all
395 components simultaneously whilst allowing for (and estimating) correlations between them.
396 Response distributions for all metrics were chosen to ensure changes were estimated on similar
397 measurement scales, and because all metrics take only positive values, log response scales were
398 used for all components.
399
400 For the *Temporal comparisons: natural environmental variation* data, total abundance (N) was
401 fit with a model that assumed a lognormal distribution and identity link function, and Poisson
402 distributions with log link functions were fit to S_n, S_{PIE} and S; Poisson distributions were chosen
403 for S_n and S_{PIE} values rounded to integers based on visual assessments that showed lognormal
404 models fit to raw S_n and S_{PIE} values greatly underpredicted the density of ones in the data. For the
405 *Temporal comparisons: experimental or natural perturbations* data, S was no longer an integer
406 value after standardizing sampling effort, and all metrics were fit with models that assumed

lognormal distributions and identity link functions. Both spatial data sets were fit with models that assumed lognormal distributions and identity link functions for total abundance (N), rarefied richness (S_n) and evenness (S_{PIE}), and a Poisson distribution and log-link function for species richness (S).

The *Temporal comparisons: natural environmental variation* models included non-varying intercepts and slopes for year, and varying intercepts and slopes for studies and cells for all responses. To allow for correlations between changes in the different responses, varying study- and cell-level parameters for all responses were drawn from a single multivariate normal distribution for each level (i.e., one for studies, one for cells; see Appendix S1: *Temporal comparisons: natural environmental variation* for equations). The models fit to the *Temporal comparisons: experimental or natural perturbations* data similarly included non-varying intercepts and slopes for year, and had varying intercepts for study, site and block fitted separately for each response. For these data, correlations between changes in the different responses were modeled by drawing varying intercepts and slopes for each combination of treatment and study for all responses from a single multivariate normal distribution (see Appendix S1: *Temporal comparisons: experimental or natural perturbations* for equations).

The models fit to the *Spatial comparisons: natural environmental variation* data included non-varying intercepts for data source (i.e., CESTES and McGill). Correlations between the different responses were modeled by assuming varying intercepts and slopes (representing the reference site and departures for all other sites from the reference, respectively) for each study and response came from a single multivariate normal distribution; over-dispersion in the richness

response was modeled using an observation-level varying intercept (see Appendix S1: *Spatial comparisons: natural environmental variation* for equations). Models fit to the *Spatial comparisons: anthropogenic perturbations* data included non-varying intercepts and slopes (representing the reference [primary vegetation] category and departures from the reference for each land use category, respectively), and varying intercepts for sites and blocks were modeled separately for each response. Correlations between changes in the different responses were modeled by assuming that varying intercepts and slopes (as per the non-varying intercepts and slopes) for each combination of source and study and each response came from a single multivariate normal distribution (see Appendix S1: *Spatial comparisons: anthropogenic perturbations* for equations).

All statistical models were estimated using the Hamiltonian Monte Carlo (HMC) sampler Stan (Carpenter et al. 2017), and coded using the 'brms' package (Burkner 2017). Details of all model specifications, and the iterations and warmup periods are provided in the Appendix, as are the priors (which were weakly regularizing). Visual inspection of the HMC chains and model diagnostics (Rhat < 1.05) showed good mixing of chains and convergence, and model adequacy assessed visually using posterior predictive checks showed that the models were able to make predictions similar to the empirical data (see Appendix Figure: S1-4). Code for all analyses is available at https://github.com/sablowes/MulticomponentBioChange, and will be archived following publication.

Results

452 Temporal changes in perturbed environments had the highest percentage of assemblages with at
453 least one component trend (ΔN, ΔS_n, ΔS_{PIE}, or ΔS) that differed from zero (44%), followed by
454 spatial comparisons across land use categories (29%), temporal changes (21%) and spatial
455 comparisons in naturally varying environments (12%). Component changes that differed from
456 zero showed broadly similar patterns across datasets, with one exception: trends differing from
457 zero for multiple components were less common for spatial comparisons between assemblages in
458 naturally varying environments (Appendix S1: Figure S5).
459
460 Pairwise relationships between changing components were typically positive (i.e., had the same
461 sign), though exceptions to this general pattern were found for all data sources (Figure 3). For
462 assemblages where ΔN and ΔS_{PIE} had the same sign (though not necessarily differing statistically
463 from zero), richness changes were typically larger in magnitude (Figure 3). In contrast,
464 assemblages where ΔN and ΔS_{PIE} had opposing signs typically exhibited changes in richness that
465 were smaller in magnitude (Figure 3). This tendency for countervailing changes in abundance
466 and evenness to constrain richness changes was most apparent for spatial comparisons between
467 different land use categories (Figure 3j-l), and there was a high proportion of assemblages that
468 were growing in size ($\Delta N > 0$) but with declining species richness ($\Delta S < 0$; Figure 3j), associated
469 with declining evenness ($\Delta S_{PIE} < 0$).
470
471 The strongest relationships were found for components changing through time, and relationships
472 between richness and changes in the SAD -- rarefied richness (Figs. 3b, e) and evenness (Figs.
473 3c, f; Figs. 4a, b) -- were stronger than those between changes in richness and total abundance
474 (Figs. 3a, c; Figs. 4a, b). Spatial comparisons had generally weak relationships overall. No strong

475 relationships between changing components emerged for comparisons in natural environments
476 (Figs. 3g-i; Fig. 4c), and only weakly positive relationships between changes in abundance,
477 evenness and richness were found in comparisons between primary vegetation and different land
478 use categories (Figure 3j-l, Figure 4d).
479
480 Temporal changes in naturally varying assemblages were roughly centered on zero for all
481 metrics (Figure 3a-c). Across assemblages, altered numbers of individuals and species richness
482 changes had a moderately positive relationship (Figure 4a), weakened predominantly by
483 assemblages that had opposing abundance and evenness relationships (Figure 3a). In contrast,
484 relationships between changes in species richness and rarefied richness, and between richness
485 changes and evenness changes were strong (Figure 4a). Assemblages in perturbed environments
486 had slightly positive temporal trends on average in all components (Figure 3d-f). Across
487 assemblages, ΔS and ΔN (Figure 3d, 4b) and ΔS and ΔS_{PIE} (Figure 3f, 4b) had relatively weak
488 positive relationships, whereas ΔS and ΔS_n (Figure 3e, 4b) showed a strong positive relationship.
489
490 Spatial comparisons in naturally varying environments exhibited highly heterogeneous patterns
491 of change centered around zero for all metrics (Figure 3g-i). Decoupled component changes
492 meant that relationships between them were generally absent or weak across assemblages (Figure
493 4c). Spatial comparisons between assemblages in primary vegetation versus those in different
494 land use categories were also highly heterogeneous, though there were typically fewer
495 individuals, less even assemblages and fewer species relative to primary vegetation (Figure 3j-l).
496 Across assemblages, land use change was typically associated with relatively weak positive
497 relationships between changes in the components of local diversity (Figure 4d).
498

Discussion

Our conceptual overview using individual-based rarefaction curves clearly shows how the expectation of positive pairwise relationships between changes in abundance, evenness and richness arises. If curves stretch or contract, we expect positive relationships between changes in total abundance and richness. Similarly, if curves flex upwards or downwards, positive relationships between changes in evenness and richness are expected. Rarefaction curves also show how contrasting signs of changes in abundance and evenness can strongly determine the magnitude of richness changes, and determine whether positive relationships between changes in richness and the other components (abundance and evenness) are likely. Both these predictions were generally well supported by our empirical analyses. Relationships between changes in abundance, evenness and richness were generally positive, and richness changes were typically greater for assemblages with strictly positive pairwise relationships. Countervailing changes in total abundance and evenness, where found, often constrained the magnitude of changes in species richness, and acted to weaken relationships between ΔN and ΔS, and ΔS_{PIE} and ΔS. Spatial comparisons had the most heterogeneous relationships between changes in abundance, evenness, and richness, and in relatively natural environments changes were sufficiently decoupled that no strong relationships emerged across assemblages. In contrast, strong positive correlations between temporal changes in species richness (ΔS) and changes in metrics associated with altered SADs (ΔS_n, ΔS_{PIE}) emerged across assemblages. These temporal results show strong support for the prediction that variation in relative abundances can dominate local variation in biodiversity (Chapin et al. 2000), even when human impacts are less direct.

Variation in assemblage size does not dominate local diversity change

522 Overall, only ~2% of assemblages in this study (22 of 1125) had changes consistent with a
523 strong 'sampling' effect on changes in species richness (i.e., ΔN & ΔS having the same sign, and
524 being the only changes different from zero). This finding complements existing evidence
525 showing that despite many tests, empirical evidence for the more-individuals hypothesis
526 (Srivastava & Lawton 1998) remains equivocal (Storch et al 2018, Vagle & McCain 2020).
527 While both (species-level) population variability and variation associated with sampling (Vagle
528 & McCain 2020) likely contribute to the weak response of species richness to variation in the
529 total number of individuals, our results are broadly consistent with previous syntheses showing
530 that broad-scale spatial variation in richness was rarely driven simply by variation in the numbers
531 of individuals (Currie et al. 2004, Storch et al 2018). Our results indicate that variation in local
532 diversity, through time or from site-to-site, is not due to changes in assemblage size passively
533 sampling more or less from a static SAD. Instead, we show that variation in local biodiversity
534 can be strongly influenced by changes to species' relative abundances. These changes can be
535 occurring at multiple scales (Hillebrand et al. 2008, Blowes et al. 2020), and could reflect altered
536 local environmental conditions (e.g., altered resource or habitat availability and diversity,
537 eutrophication, local harvest or exploitation), or changes at broader scales that alter the species
538 pool (via species additions or subtractions).
539
540 Our general result showing that variation in the total abundance of an assemblage through time
541 or space is often decoupled from changes in metrics of biodiversity such as species richness also
542 cautions against making "apples to oranges" comparisons in the context of quantifying
543 biodiversity change. For example, some estimates of change are based on either population-level
544 abundance (e.g., Living Planet Index, WWF 2020), or assemblage-level abundance (e.g., insect

545 declines; Wagner 2000, van Klink et al. 2020), whereas other change estimates are based on
546 patterns of the number or identity of species present (e.g., Dornelas et al. 2014, Newbold et al.
547 2015). Our results show that assuming abundance and richness changes are strongly correlated
548 will often be an oversimplification. Moreover, the importance of altered relative abundances for
549 local biodiversity variation means that biodiversity change estimates will frequently depend on
550 whether changes in species relative abundances influence the metrics used (see e.g., Antão et al.
551 2020b).
552
553 *Contrasting component relationships between temporal changes versus spatial comparisons of*
554 *biodiversity*
555 Relationships between changing components of biodiversity showed strikingly different patterns
556 between temporal changes and spatial comparisons. Moreover, these differences were generally
557 greater than those found between naturally-varying and perturbed assemblages, for either
558 temporal changes or spatial comparisons.
559
560 Pairwise relationships between changes in abundance, evenness and richness were typically
561 weak for spatial comparisons. Decoupling was greatest, and pairwise relationships weakest, for
562 changes between sites experiencing relatively natural environmental variation. However, given
563 our simple conceptual framework shows that some degree of interdependence cannot be avoided,
564 we caution against overinterpreting the relative independence of these component changes, and
565 further analyses examining component change relationships along continuous spatial gradients
566 are warranted. Indeed, evenness and richness are never numerically independent (Jost 2010), and
567 the weak overall relationship between changes in richness and evenness for these data was in

568 part due to assemblages with countervailing changes in abundance and evenness. Most
569 importantly, these highly variable component changes further emphasize the need for a holistic
570 approach to quantifying biodiversity change (Chase et al. 2018, Avolio et al. 2021).
571
572 Our prediction that the signs of changes in abundance and evenness can strongly determine the
573 magnitude of richness changes was most evident in the spatial contrasts between primary
574 vegetation and other land use categories (Newbold et al. 2015, 2020). Assemblages with the
575 greatest declines in abundance and evenness had the greatest richness declines. In contrast, when
576 abundance and evenness changes had opposing signs, richness changes were tempered. Indeed,
577 countervailing abundance and evenness changes were frequently associated with components
578 other than species richness (i.e., ΔN, ΔS_n, and/or ΔS_{PIE}) having a trend that differed from zero
579 across all data sources (Appendix S1: Table S1). This highlights that even apparently decoupled
580 or weakly correlated component changes have interdependencies that can remain important
581 determinants of observed changes.
582
583 In contrast to assemblage change between sites, there was strong coupling between species
584 richness and SAD changes through time. In particular, the strength of the relationship between
585 ΔS_n and ΔS resulted in estimates of change being similar for most assemblage time series in
586 relatively natural environments (Figure 3b). In some cases, this occurred despite countervailing
587 changes in total abundance and evenness (Figure 3a, b). For assemblages where abundance and
588 evenness changed in the same direction, similar estimates of ΔS_n and ΔS indicate that abundance
589 changes were occurring along a relatively flat region of the individual-based rarefaction curve.
590 This shows that changes to the total number of individuals need not strongly influence species

591 richness, even where signs are the same and they have a positive relationship. The strong
592 association between richness changes and altered relative abundances has important implications
593 for examining causes and/or consequences of biodiversity change (Hillebrand et al. 2008,
594 Crowder et al. 2010). Even where the expected positive relationships between abundance,
595 evenness and richness are found, we can more fully understand assemblage changes when all
596 component changes are examined simultaneously.
597
598 While both approaches, time series and spatial comparisons (or space-for-time substitutions),
599 have contributed to our understanding of biodiversity change, the relative merits of each for our
600 understanding of ecological dynamics has not been discussed much (Adler et al. 2020). The
601 largely decoupled component changes found here for spatial comparisons suggest that too much
602 focus on average changes across assemblages, such as those in total abundance or in species
603 richness, risks masking highly heterogeneous changes occurring within assemblages in multiple
604 components. Moreover, decoupled, heterogeneous component changes complicate using spatial
605 comparisons to infer temporal changes. The smaller effect sizes found here for time series
606 indicates greater inertia compared to site-to-site variation. More generally, the strong role of
607 changes to the SAD for variation in local biodiversity suggests that deepening our understanding
608 of altered patterns of relative abundance across scales represents an important direction for future
609 theoretical and empirical work. Here our focus has been on numerical relationships between
610 component changes, and using process-based models (e.g., Thompson et al. 2020) to examine
611 how altered metacommunity dynamics impact patterns of relative abundance across scales could
612 help our understanding how different processes impact component relationships. Similarly,
613 empirical studies could ask whether local environmental changes are affecting evenness, or if

614 changes occurring at broader spatial scales are impacting the size of species pool and the
615 regional SAD?
616
617 *Conclusions*
618 We found strong correlations between changes in the SAD and species richness changes through
619 time, whereas relationships between abundance and richness changes for both temporal and
620 spatial diversity variation were generally weak. Our findings confirm that altered species relative
621 abundances, and/or changes to the size of the species pool, often strongly influence local
622 diversity change (Chapin et al. 2010), even where human impacts are less direct. However, our
623 results also reinforce cautions against examining changes to any one component of biodiversity
624 change in isolation (e.g., Wilsey et al. 2005, Chase et al. 2018, Avolio et al. 2021).
625
626 To be most useful, quantifying (co)variation in the different components of biodiversity needs to
627 be done coherently. Individual-based rarefaction curves and associated metrics can provide an
628 intuitive and illustrative characterization of relationships among changing components of local
629 biodiversity. Whilst ecologists are increasingly looking beyond species richness to quantify
630 biodiversity change (e.g., Dornelas et al. 2014, Hillebrand et al. 2018), different components of
631 biodiversity and its change within assemblages are most often analyzed independently, and
632 frequently with metrics lacking conceptual unity. Conceptually and empirically, our results
633 emphasize that changes to the most frequently quantified aspects of biodiversity, including
634 changes to the numbers of individuals, and the relative abundance and total number of species
635 are highly interdependent. Examining how within-assemblage component changes covary with
636 potential drivers could reveal insights masked by independent aggregate estimates of change

637 across assemblages, and provide new information for understanding biodiversity change in the
638 Anthropocene.
639
640 **Acknowledgements**
641 SAB thanks the Biodiversity Synthesis group at iDiv for contructive feedback at various stages
642 of the project. SAB, TE, AS, and JMC were supported by the German Centre for Integrative
643 Biodiversity Research (iDiv) Halle-Jena-Leipzig, funded by the German Research Foundation
644 (FZT 118).
645
646 **References**
647 Antão, L.H., Bates, A.E., Blowes, S.A., Waldock, C., Supp, S.R., Magurran, A.E., Dornelas, M.,
648 Schipper, A.M., 2020a. Temperature-related biodiversity change across temperate marine and
649 terrestrial systems. Nature ecology & evolution 4, 927–933.
650 Antão, L.H., Pöyry, J., Leinonen, R., Roslin, T., 2020b. Contrasting latitudinal patterns in
651 diversity and stability in a high-latitude species-rich moth community. Global Ecology and
652 Biogeography 29, 896–907.
653 Avolio, M.L., Komatsu, K.J., Collins, S.L., Grman, E., Koerner, S.E., Tredennick, A.T., Wilcox,
654 K.R., Baer, S., Boughton, E.H., Britton, A.J., 2021. Determinants of community
655 compositional change are equally affected by global change. Ecology Letters 24, 1892–1904.
656 Blowes, S.A., Chase, J.M., Di Franco, A., Frid, O., Gotelli, N.J., Guidetti, P., Knight, T.M., May,
657 F., McGlinn, D.J., Micheli, F., 2020. Mediterranean marine protected areas have higher
658 biodiversity via increased evenness, not abundance. Journal of Applied Ecology 57, 578–589.

659 Blowes, S.A., Supp, S.R., Antão, L.H., Bates, A., Bruelheide, H., Chase, J.M., Moyes, F.,
660 Magurran, A., McGill, B., Myers-Smith, I.H., Winter, M., Bjorkman, A.D., Bowler, D.E.,
661 Byrnes, J.E., Gonzalez, A., Hines, J., Isbell, F., Jones, H.P., Navarro, L.M., Thompson, P.L.,
662 Vellend, M., Waldock, C., Dornelas, M., 2019. The geography of biodiversity change in
663 marine and terrestrial assemblages. Science 366, 339–345.
664 Bolker, B.M., 2008. Ecological models and data in R. Princeton University Press.
665 Bürkner, P.-C., 2017. brms: An R package for Bayesian multilevel models using Stan. Journal of
666 Statistical Software 80, 1–28.
667 Carpenter, B., Gelman, A., Hoffman, M.D., Lee, D., Goodrich, B., Betancourt, M., Brubaker,
668 M., Guo, J., Li, P., Riddell, A., 2017. Stan: A probabilistic programming language. Journal of
669 Statistical Software 76.
670 Caswell, H., 1976. Community structure: a neutral model analysis. Ecological monographs 46,
671 327–354.
672 Cayuela, L., Gotelli, N.J., Colwell, R.K., 2015. Ecological and biogeographic null hypotheses for
673 comparing rarefaction curves. Ecological Monographs 85, 437–455.
674 Chao, A., Gotelli, N.J., Hsieh, T.C., Sander, E.L., Ma, K.H., Colwell, R.K., Ellison, A.M., n.d.
675 Rarefaction and extrapolation with Hill numbers: a framework for sampling and estimation in
676 species diversity studies. Ecology 84, 45–67.
677 Chao, A., Jost, L., 2012. Coverage-based rarefaction and extrapolation: standardizing samples by
678 completeness rather than size. Ecology 93, 2533–2547.
679 Chapin Iii, F.S., Zavaleta, E.S., Eviner, V.T., Naylor, R.L., Vitousek, P.M., Reynolds, H.L.,
680 Hooper, D.U., Lavorel, S., Sala, O.E., Hobbie, S.E., 2000. Consequences of changing
681 biodiversity. Nature 405, 234–242.

682 Chase, J.M., Blowes, S.A., Knight, T.M., Gerstner, K., May, F., 2020. Ecosystem decay
683 exacerbates biodiversity loss with habitat loss. Nature 584, 238–243.
684 Chase, J.M., Knight, T.M., 2013. Scale-dependent effect sizes of ecological drivers on
685 biodiversity: why standardised sampling is not enough. Ecol Lett 16, 17–26.
686 Chase, J.M., McGill, B.J., McGlinn, D.J., May, F., Blowes, S.A., Xiao, X., Knight, T.M.,
687 Purschke, O., Gotelli, N.J., 2018. Embracing scale-dependence to achieve a deeper
688 understanding of biodiversity and its change across communities. Ecol Lett 21, 1737–1751.
689 Chase, J.M., McGill, B.J., Thompson, P.L., Antão, L.H., Bates, A.E., Blowes, S.A., Dornelas,
690 M., Gonzalez, A., Magurran, A.E., Supp, S.R., Winter, M., Bjorkman, A.D., Bruelheide, H.,
691 Byrnes, J.E., Sarmento Cabral, J., Elahi, R., Gomez, C., Guzman, H.M., Isbell, F., Myers-
692 Smith, I.H., Jones, H.P., Hines, J., Vellend, M., Waldock, C., O'Connor, M., 2019. Species
693 richness change across spatial scales. Oikos 1–13.
694 Coleman, B.D., Mares, M.A., Willig, M.R., Hsieh, Y.-H., 1982. Randomness, area, and species
695 richness. Ecology 63, 1121–1133.
696 Connell, J.H., 1978. Diversity in tropical rain forests and coral reefs. Science 199, 1302–1310.
697 Connor, E.F., McCoy, E.D., 1979. The statistics and biology of the species-area relationship. The
698 American Naturalist 113, 791–833.
699 Crowder, D.W., Northfield, T.D., Strand, M.R., Snyder, W.E., 2010. Organic agriculture
700 promotes evenness and natural pest control. Nature 466, 109–112.
701 Currie, D.J., 1991. Energy and large-scale patterns of animal-and plant-species richness. Am Nat
702 27–49.

703 Currie, D.J., Mittelbach, G.G., Cornell, H.V., Field, R., Guégan, J.-F., Hawkins, B.A., Kaufman,
704 D.M., Kerr, J.T., Oberdorff, T., O'Brien, E., 2004. Predictions and tests of climate-based
705 hypotheses of broad-scale variation in taxonomic richness. Ecology letters 7, 1121–1134.
706 Daskalova, G.N., Myers-Smith, I.H., Bjorkman, A.D., Blowes, S.A., Supp, S.R., Magurran,
707 A.E., Dornelas, M., 2020a. Landscape-scale forest loss as a catalyst of population and
708 biodiversity change. Science 368, 1341–1347.
709 Daskalova, G.N., Myers-Smith, I.H., Godlee, J.L., 2020b. Rare and common vertebrates span a
710 wide spectrum of population trends. Nature Communications 4394.
711 Díaz, S., Settele, J., Brondízio, E.S., Ngo, H.T., Agard, J., Arneth, A., Balvanera, P., Brauman,
712 K.A., Butchart, S.H., Chan, K.M., 2019. Pervasive human-driven decline of life on Earth
713 points to the need for transformative change. Science 366.
714 Dornelas, M., Antao, L.H., Moyes, F., Bates, A.E., Magurran, A.E., Adam, D., Akhmetzhanova,
715 A.A., Appeltans, W., Arcos, J.M., Arnold, H., 2018. BioTIME: A database of biodiversity
716 time series for the Anthropocene. Glob Ecol Biogeogr 27, 760–786.
717 Dornelas, M., Gotelli, N.J., McGill, B., Shimadzu, H., Moyes, F., Sievers, C., Magurran, A.E.,
718 2014. Assemblage time series reveal biodiversity change but not systematic loss. Science 344,
719 296–299.
720 Dornelas, M., Gotelli, N.J., Shimadzu, H., Moyes, F., Magurran, A.E., McGill, B.J., 2019. A
721 balance of winners and losers in the Anthropocene. Ecol Lett 22, 847–854.
722 Fisher, R.A., Corbet, A.S., Williams, C.B., 1943. The relation between the number of species
723 and the number of individuals in a random sample of an animal population. The Journal of
724 Animal Ecology 42–58.
725 Gaston, K.J., 2000. Global patterns in biodiversity. Nature 405, 220–227.

726 Gotelli, N.J., Colwell, R.K., 2001. Quantifying biodiversity: procedures and pitfalls in the
727 measurement and comparison of species richness. Ecol Lett 4, 379–391.
728 He, F., Legendre, P., 2002. Species diversity patterns derived from species–area models. Ecology
729 83, 1185–1198.
730 Hill, M.O., 1973. Diversity and evenness: a unifying notation and its consequences. Ecology 54,
731 427–432.
732 Hillebrand, H., Bennett, D.M., Cadotte, M.W., 2008. Consequences of dominance: a review of
733 evenness effects on local and regional ecosystem processes. Ecology 89, 1510–1520.
734 Hillebrand, H., Blasius, B., Borer, E.T., Chase, J.M., Downing, J.A., Eriksson, B.K., Filstrup,
735 C.T., Harpole, W.S., Hodapp, D., Larsen, S., 2018. Biodiversity change is uncoupled from
736 species richness trends: Consequences for conservation and monitoring. Journal of Applied
737 Ecology 55, 169–184.
738 Hudson, L.N., Newbold, T., Contu, S., Hill, S.L., Lysenko, I., De Palma, A., Phillips, H.R.,
739 Alhusseini, T.I., Bedford, F.E., Bennett, D.J., 2017. The database of the Predicts (Projecting
740 responses of ecological diversity in changing terrestrial systems) project. Ecology and
741 Evolution 7, 145–188.
742 Hughes, A.R., Byrnes, J.E., Kimbro, D.L., Stachowicz, J.J., 2007. Reciprocal relationships and
743 potential feedbacks between biodiversity and disturbance. Ecology letters 10, 849–864.
744 Hurlbert, S.H., 1971. The nonconcept of species diversity: a critique and alternative parameters.
745 Ecology 52, 577–586.
746 Jeliazkov, A., Mijatovic, D., Chantepie, S., Andrew, N., Arlettaz, R., Barbaro, L., Barsoum, N.,
747 Bartonova, A., Belskaya, E., Bonada, N., 2020. A global database for metacommunity
748 ecology, integrating species, traits, environment and space. Scientific data 7, 1–15.

749 Jones, F.A., Magurran, A.E., 2018. Dominance structure of assemblages is regulated over a
750 period of rapid environmental change. Biology letters 14, 20180187.
751 Jost, L., 2007. Partitioning diversity into independent alpha and beta components. Ecology 88,
752 2427–2439.
753 Jost, L., 2006. Entropy and diversity. Oikos 113, 363–375.
754 Kreft, H., Jetz, W., Mutke, J., Kier, G., Barthlott, W., 2008. Global diversity of island floras from
755 a macroecological perspective. Ecology letters 11, 116–127.
756 Latham, R.E., Ricklefs, R.E., 1993. Global patterns of tree species richness in moist forests:
757 energy-diversity theory does not account for variation in species richness. Oikos 325–333.
758 Leung, B., Hargreaves, A.L., Greenberg, D.A., McGill, B., Dornelas, M., Freeman, R., 2020.
759 Clustered versus catastrophic global vertebrate declines. Nature 588, 267–271.
760 MacArthur, R.H., 1965. Patterns of species diversity. Biological reviews 40, 510–533.
761 Magurran, A.E., McGill, B.J., 2011. Biological diversity: frontiers in measurement and
762 assessment. Oxford University Press.
763 May, F., Gerstner, K., McGlinn, D.J., Xiao, X., Chase, J.M., 2018. mobsim: An R package for
764 the simulation and measurement of biodiversity across spatial scales. Methods in Ecology and
765 Evolution 9, 1401–1408.
766 McGill, B.J., 2011a. Linking biodiversity patterns by autocorrelated random sampling. Am J Bot
767 98, 481–502.
768 McGill, B.J., 2011b. Species abundance distributions, in: Biological Diversity: Frontiers In
769 Measurement & Assessment (Eds Magurran, A. & McGill, B.). Oxford University Press, pp.
770 105–122.

McGill, B.J., Etienne, R.S., Gray, J.S., Alonso, D., Anderson, M.J., Benecha, H.K., Dornelas, M., Enquist, B.J., Green, J.L., He, F., Hurlbert, A.H., Magurran, A.E., Marquet, P.A., Maurer, B.A., Ostling, A., Soykan, C.U., Ugland, K.I., White, E.P., 2007. Species abundance distributions: moving beyond single prediction theories to integration within an ecological framework. Ecol Lett 10, 995–1015.

McGlinn, D.J., Xiao, X., May, F., Gotelli, N.J., Engel, T., Blowes, S.A., Knight, T.M., Purschke, O., Chase, J.M., McGill, B.J., 2019. Measurement of Biodiversity (MoB): A method to separate the scale-dependent effects of species abundance distribution, density, and aggregation on diversity change. Methods in Ecology and Evolution 10, 258–269.

McKinney, M.L., Lockwood, J.L., 1999. Biotic homogenization: a few winners replacing many losers in the next mass extinction. Trends in ecology & evolution 14, 450–453.

Menge, B.A., Berlow, E.L., Blanchette, C.A., Navarrete, S.A., Yamada, S.B., 1994. The keystone species concept: variation in interaction strength in a rocky intertidal habitat. Ecological monographs 64, 249–286.

Miller, A.D., Roxburgh, S.H., Shea, K., 2011. How frequency and intensity shape diversity–disturbance relationships. Proceedings of the National Academy of sciences 108, 5643–5648.

Mittelbach, G.G., Steiner, C.F., Scheiner, S.M., Gross, K.L., Reynolds, H.L., Waide, R.B., Willig, M.R., Dodson, S.I., Gough, L., 2001. What is the observed relationship between species richness and productivity? Ecology 82, 2381–2396.

Newbold, T., Hudson, L.N., Contu, S., Hill, S.L., Beck, J., Liu, Y., Meyer, C., Phillips, H.R., Scharlemann, J.P., Purvis, A., 2018. Widespread winners and narrow-ranged losers: Land use homogenizes biodiversity in local assemblages worldwide. PLoS biology 16, e2006841.

793 Newbold, T., Hudson, L.N., Hill, S.L., Contu, S., Lysenko, I., Senior, R.A., Börger, L., Bennett,
794 D.J., Choimes, A., Collen, B., 2015. Global effects of land use on local terrestrial biodiversity.
795 Nature 520, 45–50.
796 Newbold, T., Oppenheimer, P., Etard, A., Williams, J.J., 2020. Tropical and Mediterranean
797 biodiversity is disproportionately sensitive to land-use and climate change. Nature Ecology &
798 Evolution 4, 1630–1638.
799 Olszewski, T.D., 2004. A unified mathematical framework for the measurement of richness and
800 evenness within and among multiple communities. Oikos 104, 377–387.
801 Paine, R.T., 1974. Intertidal community structure. Oecologia 15, 93–120.
802 Palmer, M.W., Clark, D.B., Clark, D.A., 2000. Is the number of tree species in small tropical
803 forest plots nonrandom? Community Ecology 1, 95–101.
804 Preston, F.W., 1962. The canonical distribution of commonness and rarity: Part I. Ecology 43,
805 185–215.
806 Rosenberg, K.V., Dokter, A.M., Blancher, P.J., Sauer, J.R., Smith, A.C., Smith, P.A., Stanton,
807 J.C., Panjabi, A., Helft, L., Parr, M., 2019. Decline of the North American avifauna. Science
808 366, 120–124.
809 Rosenzweig, M.L., 1995. Species diversity in space and time. Cambridge University Press.
810 Scheiner, S.M., Willig, M.R., 2005. Developing unified theories in ecology as exemplified with
811 diversity gradients. The American Naturalist 166, 458–469.
812 Shmida, A.V.I., Wilson, M.V., 1985. Biological determinants of species diversity. Journal of
813 biogeography 1–20.
814 Soininen, J., Passy, S., Hillebrand, H., 2012. The relationship between species richness and
815 evenness: a meta-analysis of studies across aquatic ecosystems. Oecologia 169, 803–809.

816 Srivastava, D.S., Lawton, J.H., 1998. Why more productive sites have more species: an
817 experimental test of theory using tree-hole communities. The American Naturalist 152, 510–
818 529.
819 Stirling, G., Wilsey, B., 2001. Empirical relationships between species richness, evenness, and
820 proportional diversity. The American Naturalist 158, 286–299.
821 Storch, D., Bohdalková, E., Okie, J., 2018. The more-individuals hypothesis revisited: the role of
822 community abundance in species richness regulation and the productivity–diversity
823 relationship. Ecol Lett 21, 920–937.
824 Tilman, D., 1982. Resource competition and community structure. Princeton University Press.
825 Vagle, G.L., McCain, C.M., n.d. Natural population variability may be masking the more-
826 individuals hypothesis. Ecology 101, e03035.
827 Van Klink, R., Bowler, D.E., Gongalsky, K.B., Swengel, A.B., Gentile, A., Chase, J.M., 2020.
828 Meta-analysis reveals declines in terrestrial but increases in freshwater insect abundances.
829 Science 368, 417–420.
830 Vilà, M., Espinar, J.L., Hejda, M., Hulme, P.E., Jarošík, V., Maron, J.L., Pergl, J., Schaffner, U.,
831 Sun, Y., Pyšek, P., 2011. Ecological impacts of invasive alien plants: a meta-analysis of their
832 effects on species, communities and ecosystems. Ecology letters 14, 702–708.
833 Wagner, D.L., 2020. Insect declines in the Anthropocene. Annual review of entomology 65,
834 457–480.
835 Whittaker, R.J., Willis, K.J., Field, R., 2001. Scale and species richness: towards a general,
836 hierarchical theory of species diversity. Journal of biogeography 28, 453–470.
837 Wright, D.H., 1983. Species-energy theory: an extension of species-area theory. Oikos 496–506.

838 WWF, 2020. Living Planet Report 2020-Bending the curve of biodiversity loss. World Wildlife
839 Fund, Gland, Switzerland.
840 Zhang, Y., Chen, H.Y., Reich, P.B., 2012. Forest productivity increases with evenness, species
841 richness and trait variation: a global meta-analysis. Journal of ecology 100, 742–749.
842

Figure 1: (a) Individual-based rarefaction (IBR) curves for two hypothetical assemblages, showing the four components we use to quantify change (N, S, S_n, PIE). We visualize relationships between these four components of the IBR curve by plotting: (b) changes in species richness (ΔS) as a function of altered numbers of individuals (ΔN), (c) changes in species richness (ΔS) as a function of changes in rarefied richness (ΔS_n), and (d) changes in species richness (ΔS) as a function of the numbers equivalent conversion of the Probability of Interspecific Encounter (ΔS_{PIE}). We show ΔPIE on the figure to illustrate changes of the PIE (it is equivalent to the slope at the base of the curve) with the IBR, but use the numbers equivalent transformation (ΔS_{PIE}) in all analyses. Points on panels (b, c, and d) show changes between the two hypothetical assemblages, with the reference assemblage depicted by the grey line.

Figure 2: Conceptual illustrations of potential pathways of local assemblage diversity change and corresponding relationships between component changes. Starting from a reference assemblage (depicted with grey rarefaction curves), diversity change can be due to (a) more individuals only, (b) changes to the species abundance distribution only (e.g., increased species pool size or increased evenness), or (c) changes in total abundance and the SAD that result in positive pairwise relationships between ΔN, ΔS_n, ΔS_{PIE}, and ΔS. However, if the signs of ΔN and ΔS_{PIE} differ, their relationships with ΔS weaken and species richness can (d) remain static, (e) decrease or (f) increase. We visualize pairwise relationships between component changes for each scenario (i.e., the different shaped symbols) using: (g) changes in species richness as a function of changes to the number of individuals, (h) changes in species richness as a function of changes in rarefied richness, and (i) changes in species richness as a function of changes in evenness.

866 **Figure 3**: Empirical relationships between four components of local diversity change. Change in
867 species richness as a function of changes in the numbers of individuals (left column), rarefied
868 richness (middle column), and evenness (right column) for (a-c) study-level estimates of
869 temporal changes in naturally varying environments; (d-f) estimates of temporal change for
870 combinations of study and treatment in perturbed environments; (g-i) estimates of spatial
871 changes within studies from an arbitrary reference site along natural environmental gradients;
872 and, (j-l) estimates of spatial change within studies between primary vegetation and different
873 land use categories. Colored concentration ellipses show the confidence interval (5 and 95%) of
874 the posterior distributions. Dotted grey lines are x and y = 0, and x = y. See Appendix S1: Figure
875 S6 for remaining pairwise relationships. Scale of x- and y-axes vary between panels; one
876 estimate with $\Delta\log(N) = -1.79$, $\Delta\log(S) = -3.77$, $\Delta\log(S_n) = -3.23$, $\Delta\log(S_{PIE}) = -3.21$, removed
877 from (j-l) for clarity.
878
879 **Figure 4**: Component correlations among studies within each data source. Density plots for the
880 posterior distribution of pairwise correlations between component changes for (a) temporal
881 comparison in naturally varying environments, (b) temporal comparisons in perturbed
882 environments, (c) spatial comparisons along natural gradients, and (d) spatial comparisons
883 between different land use categories. Correlations estimated separately for sites and land use
884 categories relative to the references were combined on (c) and (d).
885
886

887 Figure 1

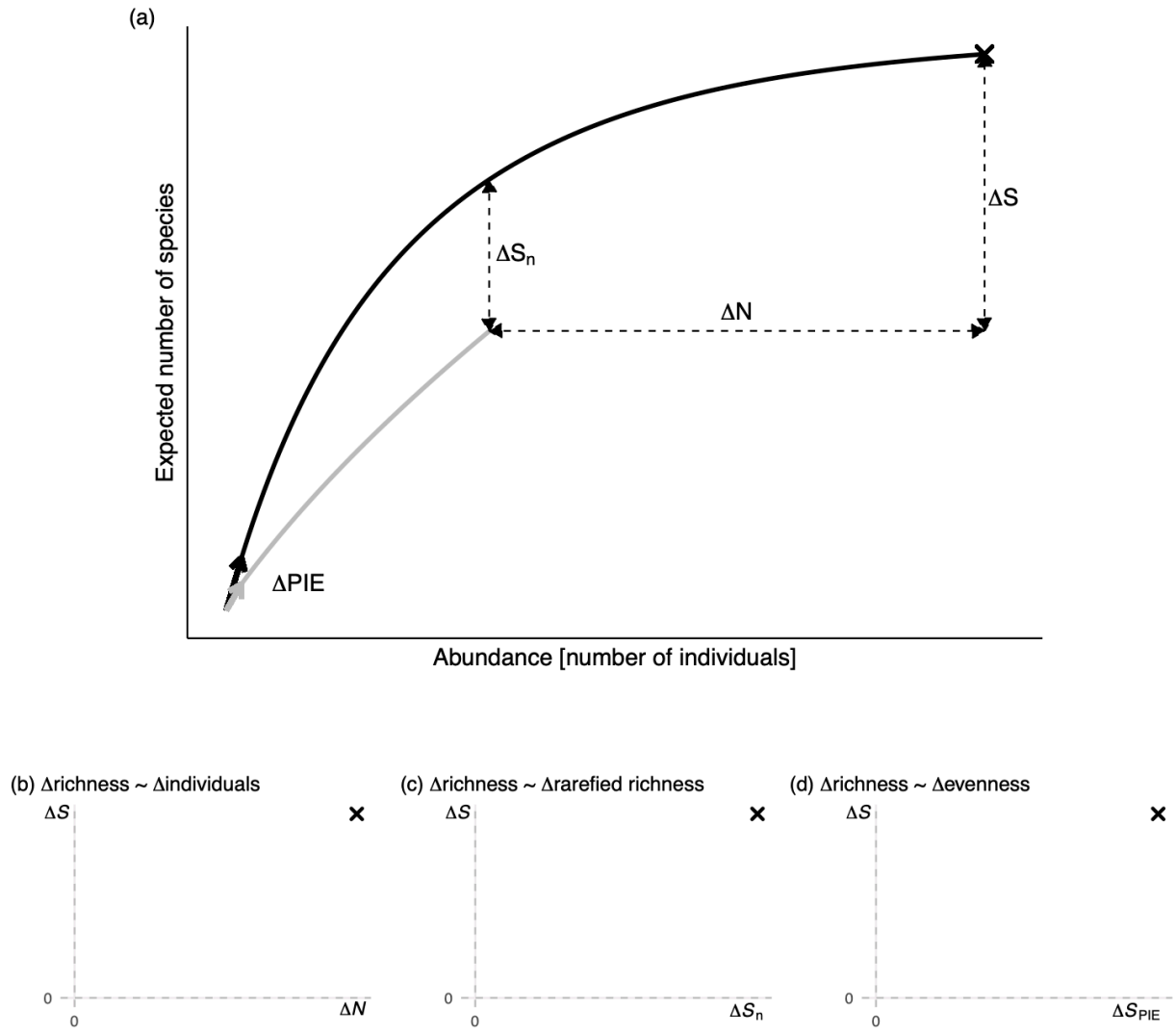

888

889 Figure 2

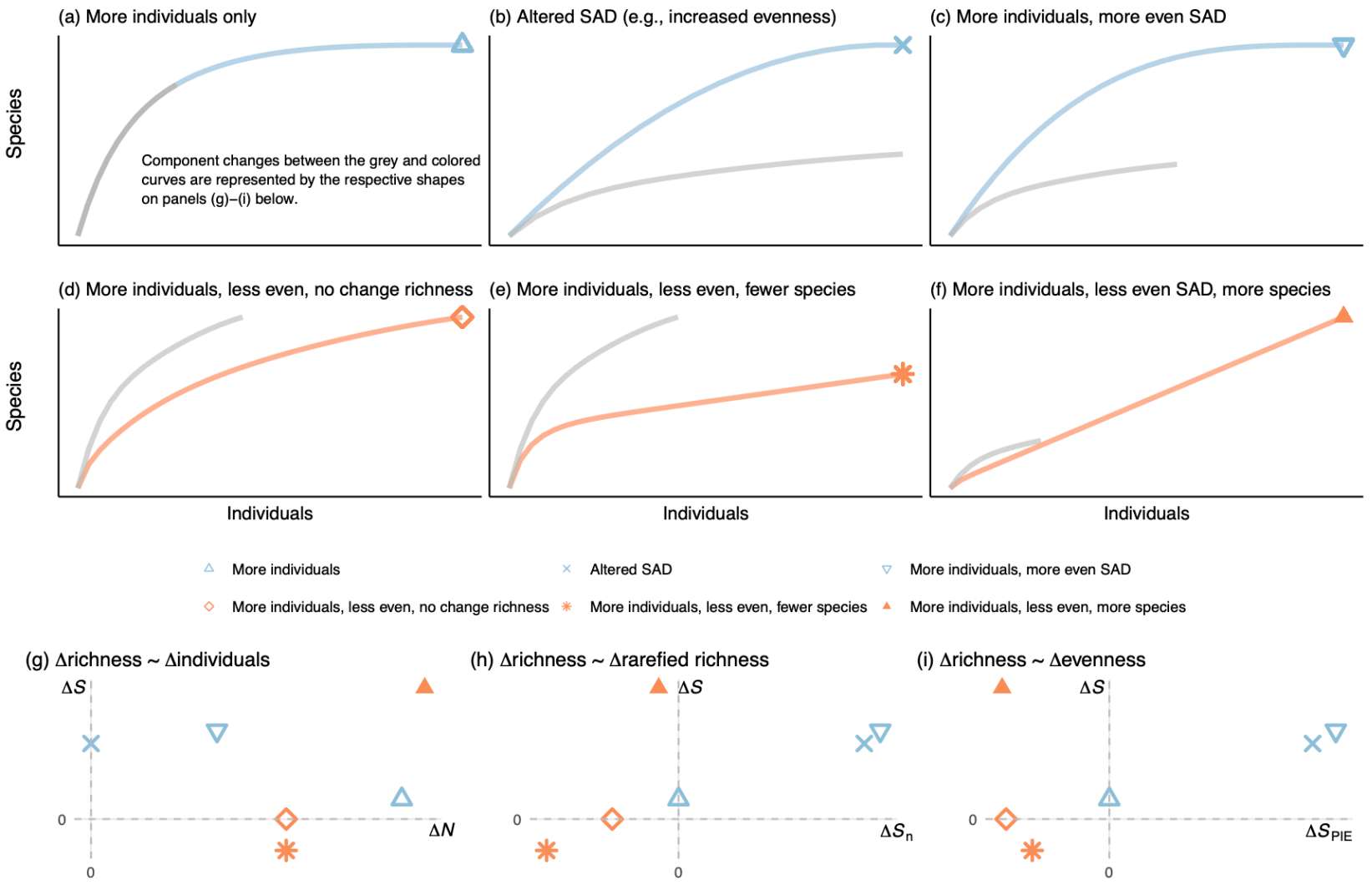

890

891 Figure 3

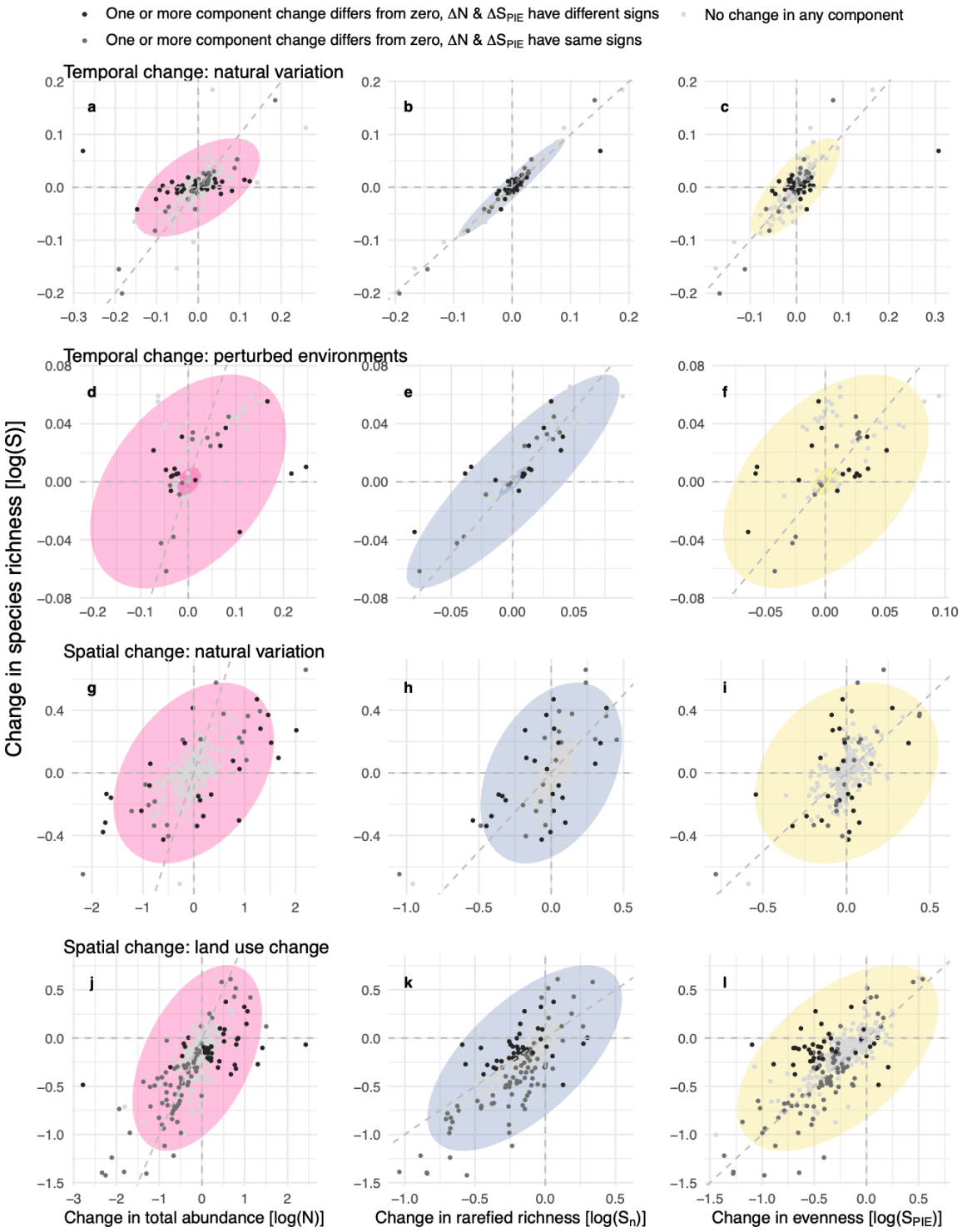

892

893

894 Figure 4

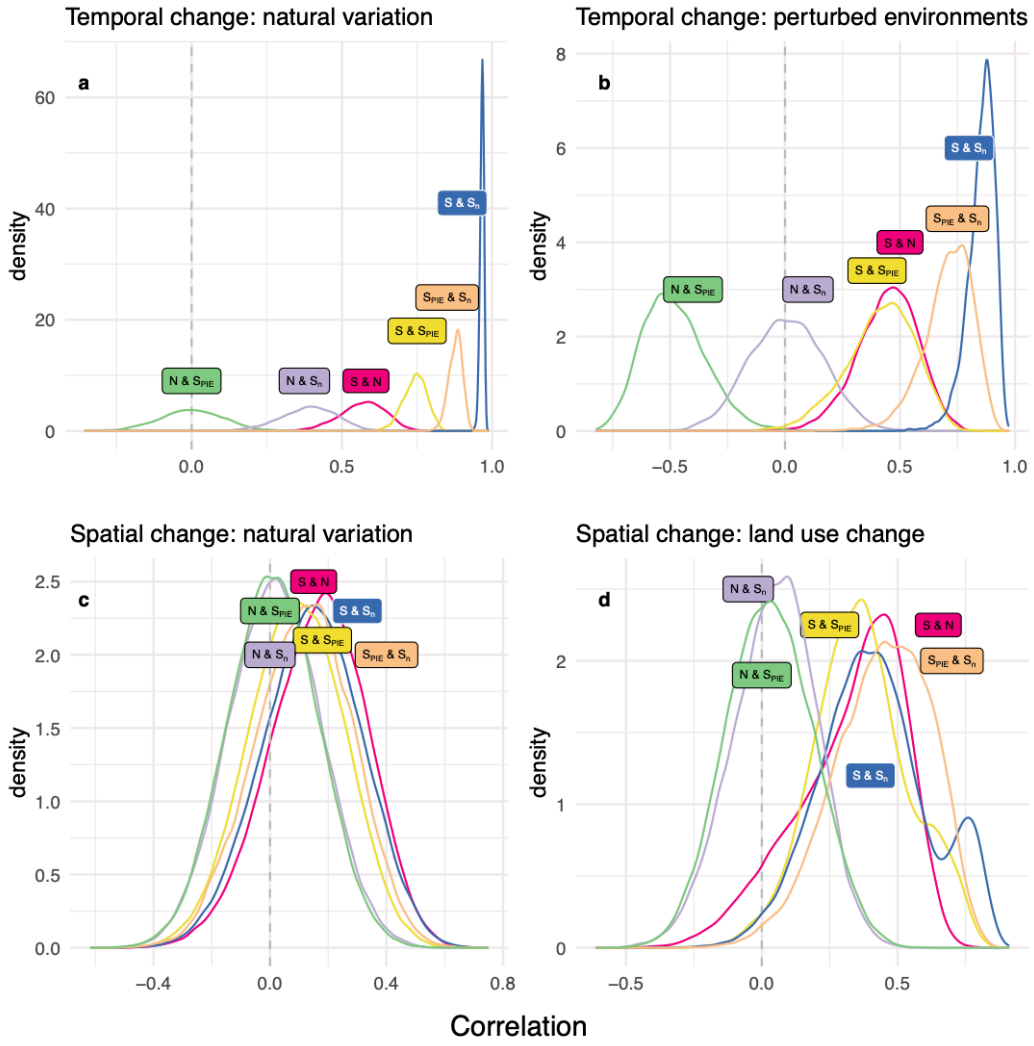

895
896

Appendix S1

Title: Local biodiversity change reflects interactions among changing abundance, evenness and richness

Authors: Shane A. Blowes, Gergana N. Daskalova, Maria Dornelas, Thore Engel, Nicholas J. Gotelli, Anne E. Magurran, Inês S. Martins, Brian McGill, Daniel J. McGlinn, Alban Sagouis Hideyasu Shimadzu, Sarah R. Supp, Jonathan M. Chase

Journal: Ecology

Table S1: Countervailing changes in abundance (ΔN) and evenness (ΔS_{PIE}) often result in components other than richness changing. Component(s) with high probability of change as per Figure 2 (i.e., 90% CI does not overlap zero); each row shows the number of assemblages with either countervailing [sign(ΔN) x sign(ΔS_{PIE}) = -1] or abundance and evenness changes with the same direction [sign(ΔN) x sign(ΔS_{PIE}) = 1] for the different data sources.

		Temporal change: natural variation	**Temporal change: perturbed environments**	**Spatial change: natural variation**	**Spatial change: land use change**
Component with high probability of change	sign(ΔN) x sign(ΔS_{PIE})	Number of assemblages	Number of assemblages	Number of assemblages	Number of assemblages
None	-1	97	23	154	107
None	1	131	12	214	191
N only	-1	7	0	7	5
N only	1	2	1	3	5
S_{PIE} only	-1	6	0	1	10
S_{PIE} only	1	2	0	2	12
S_n only	-1	0	1	7	1
S_n only	1	1	1	3	0
S only	-1	1	0	2	1
S only	1	1	0	5	6
S & S_n	-1	0	0	1	1

S & S_n	1	6	2	3	6
S & S_{PIE}	-1	0	0	0	0
S & S_{PIE}	1	1	0	1	3
S & N	-1	1	3	0	3
S & N	1	0	1	3	10
S_n & S_{PIE}	-1	3	4	2	9
S_n & S_{PIE}	1	0	0	0	1
S_n & N	-1	0	0	1	1
S_n & N	1	0	1	0	0
N & S_{PIE}	-1	4	0	0	3
N & S_{PIE}	1	0	0	0	0
S_n, N & S_{PIE}	-1	3	4	0	6
S_n, N & S_{PIE}	1	0	0	0	0
S, N & S_{PIE}	-1	2	0	0	0
S, N & S_{PIE}	1	1	0	0	4
S, S_n, N & S_{PIE}	-1	7	4	0	2
S, S_n, N & S_{PIE}	1	12	6	1	31

Temporal comparisons: natural environmental variation

We fit a model that assumed a lognormal distribution for total abundance (N), and poisson distributions (with log link functions) for species richness (S), rarefied richness (S_n) and evenness (S_{PIE}). We ran the model with four chains for 2000 iterations, with 1000 used as warmup. The model took the following form:

$$N_{ijt} \sim lognormal(\mu_{ijt}^{N}, \sigma),$$

$$S_{ijt} \sim pois(\lambda_{ijt}^{S}),$$

$$S_{n_{ijt}} \sim pois(\lambda_{ijt}^{S_n}),$$

$$S_{PIE_{ijt}} \sim pois(\lambda_{ijt}^{S_{PIE}}),$$

$$\mu_{ijt}^{N} = \beta_0^N + \beta_{0i}^N + \beta_{0ij}^N + (\beta_1^N + \beta_{1i}^N + \beta_{1ij}^N) year_{ijt},$$

$$\log(\lambda_{ijt}^{S}) = \beta_0^S + \beta_{0i}^S + \beta_{0ij}^S + (\beta_1^S + \beta_{1i}^S + \beta_{1ij}^S) year_{ijt},$$

$$\log(\lambda_{ijt}^{S_n}) = \beta_0^{S_n} + \beta_{0i}^{S_n} + \beta_{0ij}^{S_n} + (\beta_1^{S_n} + \beta_{1i}^{S_n} + \beta_{1ij}^{S_n}) year_{ijt},$$

$$\log(\lambda_{ijt}^{S_{PIE}}) = \beta_0^{S_{PIE}} + \beta_{0i}^{S_{PIE}} + \beta_{0ij}^{S_{PIE}} + (\beta_1^{S_{PIE}} + \beta_{1i}^{S_{PIE}} + \beta_{1ij}^{S_{PIE}}) year_{ijt},$$

$$\left[\beta_{0i}^N, \beta_{0i}^S, \beta_{0i}^{S_n}, \beta_{0i}^{S_{PIE}}, \beta_{1i}^N, \beta_{1i}^S, \beta_{1i}^{S_n}, \beta_{1i}^{S_{PIE}}\right]' \sim MVNormal(\mathbf{0}, \boldsymbol{SRS}),$$

$$\boldsymbol{S} = \begin{bmatrix} \sigma_{0i}^N & 0 & 0 & 0 & 0 & 0 & 0 & 0 \\ 0 & \sigma_{0i}^S & 0 & 0 & 0 & 0 & 0 & 0 \\ 0 & 0 & \sigma_{0i}^{S_n} & 0 & 0 & 0 & 0 & 0 \\ 0 & 0 & 0 & \sigma_{0i}^{S_{PIE}} & 0 & 0 & 0 & 0 \\ 0 & 0 & 0 & 0 & \sigma_{1i}^N & 0 & 0 & 0 \\ 0 & 0 & 0 & 0 & 0 & \sigma_{1i}^S & 0 & 0 \\ 0 & 0 & 0 & 0 & 0 & 0 & \sigma_{1i}^{S_n} & 0 \\ 0 & 0 & 0 & 0 & 0 & 0 & 0 & \sigma_{1i}^{S_{PIE}} \end{bmatrix},$$

$$\boldsymbol{R} = \begin{bmatrix} 1 & \rho_{N_{0i}S_{0i}} & \rho_{N_{0i}S_{n0i}} & \rho_{N_{0i}S_{PIE0i}} & \rho_{N_{0i}N_{1i}} & \rho_{N_{0i}S_{1i}} & \rho_{N_{0i}S_{n1i}} & \rho_{N_{0i}S_{PIE1i}} \\ \rho_{N_{0i}S_{0i}} & 1 & \rho_{S_{0i}S_{n0i}} & \rho_{S_{0i}S_{PIE0i}} & \rho_{S_{0i}N_{1i}} & \rho_{S_{0i}S_{1i}} & \rho_{S_{0i}S_{n1i}} & \rho_{S_{0i}S_{PIE1i}} \\ \rho_{N_{0i}S_{n0i}} & \rho_{S_{0i}S_{n0i}} & 1 & \rho_{S_{n0i}S_{PIE0i}} & \rho_{S_{n0i}N_{1i}} & \rho_{S_{n0i}S_{1i}} & \rho_{S_{n0i}S_{n1i}} & \rho_{S_{n0i}S_{PIE1i}} \\ \rho_{N_{0i}S_{PIE0i}} & \rho_{S_{0i}S_{PIE0i}} & \rho_{S_{n0i}S_{PIE0i}} & 1 & \rho_{S_{PIE0i}N_{1i}} & \rho_{S_{PIE0i}S_{1i}} & \rho_{S_{PIE0i}S_{n1i}} & \rho_{S_{PIE0i}S_{PIE1i}} \\ \rho_{N_{0i}N_{1i}} & \rho_{S_{0i}N_{1i}} & \rho_{S_{n0i}N_{1i}} & \rho_{S_{PIE0i}N_{1i}} & 1 & \rho_{N_{1i}S_{1i}} & \rho_{N_{1i}S_{n1i}} & \rho_{N_{1i}S_{PIE1i}} \\ \rho_{N_{0i}S_{1i}} & \rho_{S_{0i}S_{1i}} & \rho_{S_{n0i}S_{1i}} & \rho_{S_{PIE0i}S_{1i}} & \rho_{N_{1i}S_{1i}} & 1 & \rho_{S_{1i}S_{n1i}} & \rho_{S_{1i}S_{PIE1i}} \\ \rho_{N_{0i}S_{n1i}} & \rho_{S_{0i}S_{n1i}} & \rho_{S_{n0i}S_{n1i}} & \rho_{S_{PIE0i}S_{n1i}} & \rho_{N_{1i}S_{n1i}} & \rho_{S_{1i}S_{n1i}} & 1 & \rho_{S_{n1i}S_{PIE1i}} \\ \rho_{N_{0i}S_{PIE1i}} & \rho_{S_{0i}S_{PIE1i}} & \rho_{S_{n0i}S_{PIE1i}} & \rho_{S_{PIE0i}S_{PIE1i}} & \rho_{N_{1i}S_{PIE1i}} & \rho_{S_{1i}S_{PIE1i}} & \rho_{S_{n1i}S_{PIE1i}} & 1 \end{bmatrix},$$

$$\left[\beta_{0ij}^N, \beta_{0ij}^S, \beta_{0ij}^{S_n}, \beta_{0ij}^{S_{PIE}}, \beta_{1ij}^N, \beta_{1ij}^S, \beta_{1ij}^{S_n}, \beta_{1ij}^{S_{PIE}}\right]' \sim MVNormal(\mathbf{0}, \boldsymbol{SRS}),$$

$$\boldsymbol{S} = \begin{bmatrix} \sigma_{0ij}^{N} & 0 & 0 & 0 & 0 & 0 & 0 & 0 \\ 0 & \sigma_{0ij}^{S} & 0 & 0 & 0 & 0 & 0 & 0 \\ 0 & 0 & \sigma_{0ij}^{S_n} & 0 & 0 & 0 & 0 & 0 \\ 0 & 0 & 0 & \sigma_{0ij}^{S_{PIE}} & 0 & 0 & 0 & 0 \\ 0 & 0 & 0 & 0 & \sigma_{1ij}^{N} & 0 & 0 & 0 \\ 0 & 0 & 0 & 0 & 0 & \sigma_{1ij}^{S} & 0 & 0 \\ 0 & 0 & 0 & 0 & 0 & 0 & \sigma_{1ij}^{S_n} & 0 \\ 0 & 0 & 0 & 0 & 0 & 0 & 0 & \sigma_{1ij}^{S_{PIE}} \end{bmatrix},$$

$$R = \begin{bmatrix} 1 & \rho_{N_{0ij}S_{0ij}} & \rho_{N_{0ij}S_{n_{0ij}}} & \rho_{N_{0ij}S_{PIE_{0ij}}} & \rho_{N_{0ij}N_{1ij}} & \rho_{N_{0ij}S_{1ij}} & \rho_{N_{0ij}S_{n_{1ij}}} & \rho_{N_{0ij}S_{PIE_{1ij}}} \\ \rho_{N_{0ij}S_{0ij}} & 1 & \rho_{S_{0ij}S_{n_{0ij}}} & \rho_{S_{0ij}S_{PIE_{0ij}}} & \rho_{S_{0ij}N_{1ij}} & \rho_{S_{0ij}S_{1ij}} & \rho_{S_{0ij}S_{n_{1ij}}} & \rho_{S_{0ij}S_{PIE_{1ij}}} \\ \rho_{N_{0ij}S_{n_{0ij}}} & \rho_{S_{0ij}S_{n_{0ij}}} & 1 & \rho_{S_{n_{0ij}}S_{PIE_{0ij}}} & \rho_{S_{n_{0ij}}N_{1ij}} & \rho_{S_{n_{0ij}}S_{1ij}} & \rho_{S_{n_{0ij}}S_{n_{1ij}}} & \rho_{S_{n_{0ij}}S_{PIE_{1ij}}} \\ \rho_{N_{0ij}S_{PIE_{0ij}}} & \rho_{S_{0ij}S_{PIE_{0ij}}} & \rho_{S_{n_{0ij}}S_{PIE_{0ij}}} & 1 & \rho_{S_{PIE_{0ij}}N_{1ij}} & \rho_{S_{PIE_{0ij}}S_{1ij}} & \rho_{S_{PIE_{0ij}}S_{n_{1ij}}} & \rho_{S_{PIE_{0ij}}S_{PIE_{1ij}}} \\ \rho_{N_{0ij}N_{1ij}} & \rho_{S_{0ij}N_{1ij}} & \rho_{S_{n_{0ij}}N_{1ij}} & \rho_{S_{PIE_{0ij}}N_{1ij}} & 1 & \rho_{N_{1ij}S_{1ij}} & \rho_{N_{1ij}S_{n_{1ij}}} & \rho_{N_{1ij}S_{PIE_{1ij}}} \\ \rho_{N_{0ij}S_{1ij}} & \rho_{S_{0ij}S_{1ij}} & \rho_{S_{n_{0ij}}S_{1ij}} & \rho_{S_{PIE_{0ij}}S_{1ij}} & \rho_{N_{1ij}S_{1ij}} & 1 & \rho_{S_{1ij}S_{n_{1ij}}} & \rho_{S_{1ij}S_{PIE_{1ij}}} \\ \rho_{N_{0ij}S_{n_{1ij}}} & \rho_{S_{0ij}S_{n_{1ij}}} & \rho_{S_{n_{0ij}}S_{n_{1ij}}} & \rho_{S_{PIE_{0ij}}S_{n_{1ij}}} & \rho_{N_{1ij}S_{n_{1ij}}} & \rho_{S_{1ij}S_{n_{1ij}}} & 1 & \rho_{S_{n_{1ij}}S_{PIE_{1ij}}} \\ \rho_{N_{0ij}S_{PIE_{1ij}}} & \rho_{S_{0ij}S_{PIE_{1ij}}} & \rho_{S_{n_{0ij}}S_{PIE_{1ij}}} & \rho_{S_{PIE_{0ij}}S_{PIE_{1ij}}} & \rho_{N_{1ij}S_{PIE_{1ij}}} & \rho_{S_{1ij}S_{PIE_{1ij}}} & \rho_{S_{n_{1ij}}S_{PIE_{1ij}}} & 1 \end{bmatrix},$$

$$\beta_0^N, \beta_0^S, \beta_0^{S_n}, \beta_0^{S_{PIE}} \sim N(0, 1),$$

$$\beta_1^N, \beta_1^S, \beta_1^{S_n}, \beta_1^{S_{PIE}} \sim N(0, 0.2),$$

$$\sigma_{0i}^S, \sigma_{0i}^{S_n}, \sigma_{0i}^{S_{PIE}}, \sigma_{1i}^S, \sigma_{1i}^{S_n}, \sigma_{1i}^{S_{PIE}}, \sigma_{0ij}^S, \sigma_{0ij}^{S_n}, \sigma_{0ij}^{S_{PIE}}, \sigma_{1ij}^S, \sigma_{1ij}^{S_n}, \sigma_{1ij}^{S_{PIE}} \sim student(3, 0, 10),$$

$$\sigma, \sigma_{0i}^N, \sigma_{1ij}^N, \sigma_{0ij}^N, \sigma_{1ij}^N \sim student(3, 0, 16),$$

$$\boldsymbol{R} \sim LJK(1),$$

where N_{ijt}, S_{ijt}, $S_{n_{ijt}}$, and $S_{PIE_{ijt}}$ are the values of each of the metrics in the *j*th cell of the *i*th study in year *t*, and $year_{ijt}$ is the time in years. β_0 and β_1 (with the respective superscripts for each metric) represent the non-varying intercepts and slopes, respectively. β_{0i} and β_{1i} (with the respective superscripts for each metric) represent the varying intercepts and slopes for study-level departures from β_0 and β_1, respectively. β_{0ij} and β_{1ij} (with the respective superscripts for each metric) represent the varying intercepts and slopes for cell-level departures from β_0 and β_1, respectively. The covariance matrices of each multivariate normal distribution for varying effects (one each for the study- and cell-level departures) are parameterised in terms of a correlation matrix **R** and two matrices **S** with diagonal elements σ (superscripts for metrics, subscripts denote intercept (0), slopes (1) and level: studies *i* and cells *j*).

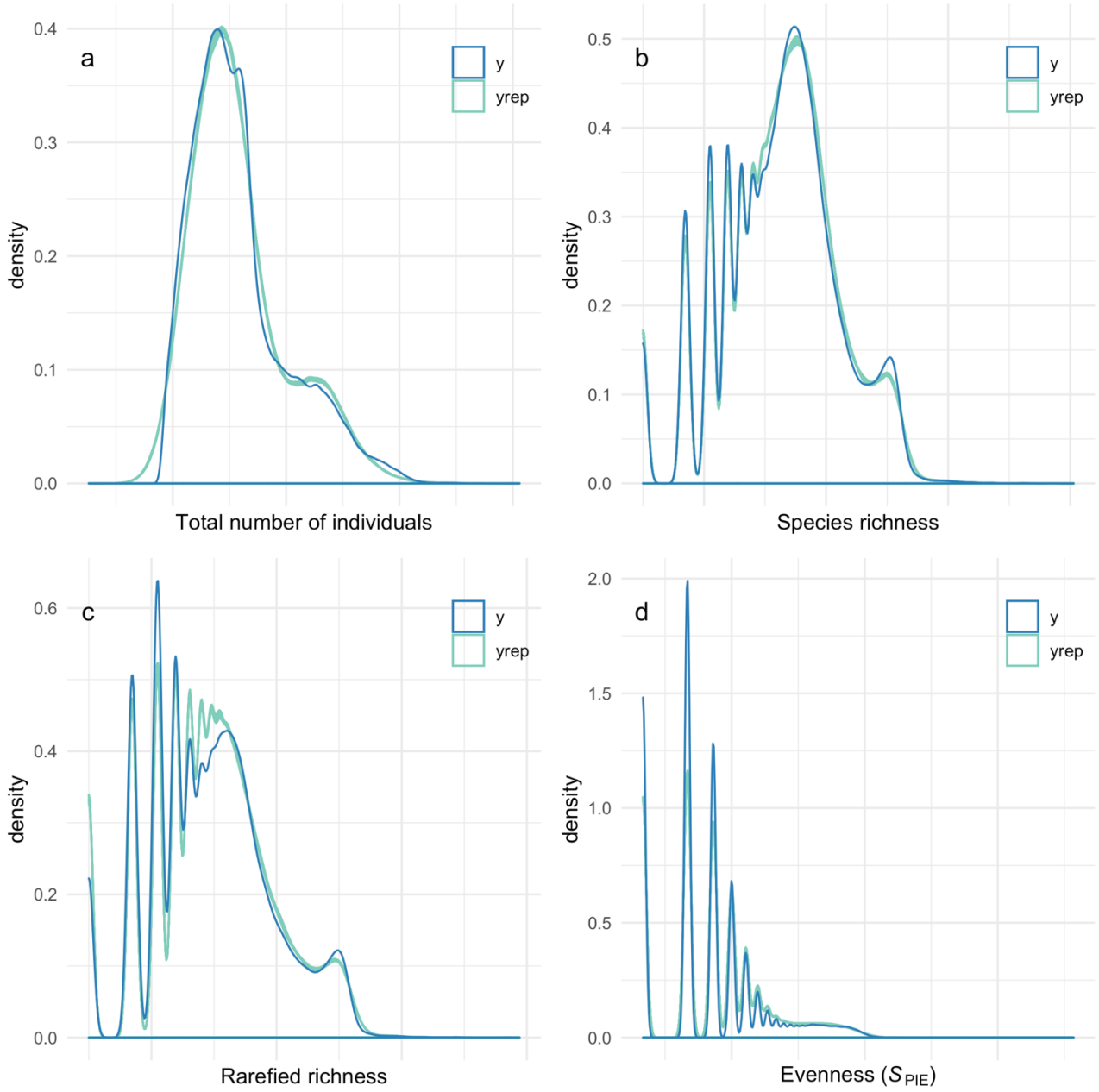

Figure S1: Posterior predictive checks for the model fit to the temporal data in naturally varying environments. (a) Total numbers of individuals, (b) species richness, (c) rarefied richness (S_n) and (d) evenness (S_{PIE}). Each panel shows the density of the data (y) and ten draws of the posterior distribution (yrep).

Temporal comparisons: experimental or natural perturbations

We fit a model that assumed lognormal distributions for all response variables (N, S, S_n, S_{PIE}). Our focus is on the treatment-level variation in the metrics, and we created a covariate that was the concatenation of study and treatment to this end. Additionally, as some studies had blocks within sites, and others did not, we created a new variable that was the concatenation of site and block, where those without block had no unique identifier. We ran the model with four chains for 3000 iterations, with 1500 used as warmup. The model took the following form:

$$N_{ijkt} \sim lognormal(\mu^N_{ijkt}, \sigma^N),$$

$$S_{ijkt} \sim lognormal(\mu^S_{ijkt}, \sigma^S),$$

$$S_{n\,ijkt} \sim lognormal(\mu^{S_n}_{ijkt}, \sigma^{S_n}),$$

$$S_{PIE\,ijkt} \sim lognormal(\mu^{S_{PIE}}_{ijkt}, \sigma^{S_{PIE}}),$$

$$\mu^N_{ijkt} = \beta^N_0 + \beta^N_{0i} + \beta^N_{0j} + \beta^N_{0k} + (\beta^N_1 + \beta^N_{1k}) year_{ijkt},$$

$$\mu^S_{ijkt} = \beta^S_0 + \beta^S_{0i} + \beta^S_{0j} + \beta^S_{0k} + (\beta^S_1 + \beta^S_{1k}) year_{ijkt},$$

$$\mu^{S_n}_{ijkt} = \beta^{S_n}_0 + \beta^{S_n}_{0i} + \beta^{S_n}_{0j} + \beta^{S_n}_{0k} + (\beta^{S_n}_1 + \beta^{S_n}_{1k}) year_{ijkt},$$

$$\mu^{S_{PIE}}_{ijkt} = \beta^{S_{PIE}}_0 + \beta^{S_{PIE}}_{0i} + \beta^{S_{PIE}}_{0j} + \beta^{S_{PIE}}_{0k} + \left(\beta^{S_{PIE}}_1 + \beta^{S_{PIE}}_{1k}\right) year_{ijkt},$$

$$\left[\beta^N_{0k}, \beta^S_{0k}, \beta^{S_n}_{0k}, \beta^{S_{PIE}}_{0k}, \beta^N_{1k}, \beta^S_{1k}, \beta^{S_n}_{1k}, \beta^{S_{PIE}}_{1k}\right]' \sim MVNormal(\mathbf{0}, \boldsymbol{SRS}),$$

$$\boldsymbol{S} = \begin{bmatrix} \sigma^N_{0k} & 0 & 0 & 0 & 0 & 0 & 0 & 0 \\ 0 & \sigma^S_{0k} & 0 & 0 & 0 & 0 & 0 & 0 \\ 0 & 0 & \sigma^{S_n}_{0k} & 0 & 0 & 0 & 0 & 0 \\ 0 & 0 & 0 & \sigma^{S_{PIE}}_{0k} & 0 & 0 & 0 & 0 \\ 0 & 0 & 0 & 0 & \sigma^N_{1k} & 0 & 0 & 0 \\ 0 & 0 & 0 & 0 & 0 & \sigma^S_{1k} & 0 & 0 \\ 0 & 0 & 0 & 0 & 0 & 0 & \sigma^{S_n}_{1k} & 0 \\ 0 & 0 & 0 & 0 & 0 & 0 & 0 & \sigma^{S_{PIE}}_{1k} \end{bmatrix},$$

$$\boldsymbol{R} = \begin{bmatrix} 1 & \rho_{N_{0k}S_{0k}} & \rho_{N_{0k}S_{n0k}} & \rho_{N_{0k}S_{PIE0k}} & \rho_{N_{0k}N_{1k}} & \rho_{N_{0k}S_{1k}} & \rho_{N_{0k}S_{n1k}} & \rho_{N_{0k}S_{PIE1k}} \\ \rho_{N_{0k}S_{0k}} & 1 & \rho_{S_{0k}S_{n0k}} & \rho_{S_{0k}S_{PIE0k}} & \rho_{S_{0k}N_{1k}} & \rho_{S_{0k}S_{1k}} & \rho_{S_{0k}S_{n1k}} & \rho_{S_{0k}S_{PIE1k}} \\ \rho_{N_{0k}S_{n0k}} & \rho_{S_{0k}S_{n0k}} & 1 & \rho_{S_{n0k}S_{PIE0k}} & \rho_{S_{n0k}N_{1k}} & \rho_{S_{n0k}S_{1k}} & \rho_{S_{n0k}S_{n1k}} & \rho_{S_{n0k}S_{PIE1k}} \\ \rho_{N_{0k}S_{PIE0k}} & \rho_{S_{0k}S_{PIE0k}} & \rho_{S_{n0k}S_{PIE0k}} & 1 & \rho_{S_{PIE0k}N_{1k}} & \rho_{S_{PIE0k}S_{1k}} & \rho_{S_{PIE0k}S_{n1k}} & \rho_{S_{PIE0k}S_{PIE1k}} \\ \rho_{N_{0k}N_{1k}} & \rho_{S_{0k}N_{1k}} & \rho_{S_{n0k}N_{1k}} & \rho_{S_{PIE0k}N_{1k}} & 1 & \rho_{N_{1k}S_{1k}} & \rho_{N_{1k}S_{n1k}} & \rho_{N_{1k}S_{PIE1k}} \\ \rho_{N_{0k}S_{1k}} & \rho_{S_{0k}S_{1k}} & \rho_{S_{n0k}S_{1k}} & \rho_{S_{PIE0k}S_{1k}} & \rho_{N_{1k}S_{1k}} & 1 & \rho_{S_{1k}S_{n1k}} & \rho_{S_{1k}S_{PIE1k}} \\ \rho_{N_{0k}S_{n1k}} & \rho_{S_{0k}S_{n1k}} & \rho_{S_{n0k}S_{n1k}} & \rho_{S_{PIE0k}S_{n1k}} & \rho_{N_{1k}S_{n1k}} & \rho_{S_{1k}S_{n1k}} & 1 & \rho_{S_{n1k}S_{PIE1k}} \\ \rho_{N_{0k}S_{PIE1k}} & \rho_{S_{0k}S_{PIE1k}} & \rho_{S_{n0k}S_{PIE1i}} & \rho_{S_{PIE0k}S_{PIE1k}} & \rho_{N_{1k}S_{PIE1k}} & \rho_{S_{1k}S_{PIE1k}} & \rho_{S_{n1k}S_{PIE1k}} & 1 \end{bmatrix},$$

$$\beta^N_0, \beta^S_0, \beta^{S_n}_0, \beta^{S_{PIE}}_0 \sim N(0, 1),$$

$$\beta^N_1, \beta^S_1, \beta^{S_n}_1, \beta^{S_{PIE}}_1 \sim N(0, 0.2),$$

$$\sigma^S_{0i}, \sigma^{S_n}_{0i}, \sigma^{S_{PIE}}_{0i}, \sigma^S_{1i}, \sigma^{S_n}_{1i}, \sigma^{S_{PIE}}_{1i}, \sigma^S_{0ij}, \sigma^{S_n}_{0ij}, \sigma^{S_{PIE}}_{0ij}, \sigma^S_{1ij}, \sigma^{S_n}_{1ij}, \sigma^{S_{PIE}}_{1ij} \sim normal(0, 1),$$

$$\sigma, \sigma^N_{0i}, \sigma^N_{1ij}, \sigma^N_{0ij}, \sigma^N_{1ij} \sim student(3, 0, 16),$$

$$\boldsymbol{R} \sim LJK(1),$$

where N_{ijkt}, S_{ijkt}, $S_{n_{ijkt}}$, and $S_{PIE_{ijkt}}$ are the values of each of the metrics in the kth study-treatment combination, for the *j*th study-block combination of the *i*th study in year *t*, and $year_{ijkt}$ is the time in years. β_0 and β_1 (with the respective superscripts for each metric) represent the non-varying intercepts and slopes, respectively. β_{0i} (with the respective superscripts for each metric) represent the varying intercepts study-level departures from β_0, and β_{0j} (with the respective superscripts for each metric) represent the varying intercepts study-block level departures from β_0. β_{0k} and β_{1k} (with the respective superscripts for each metric) represent the varying intercepts and slopes for study-treatment departures from β_0 and β_1, respectively. The covariance matrix of the multivariate normal distribution for varying study-treatment effects were parameterised in terms of a correlation matrix **R** and two matrices **S** with diagonal elements σ (superscripts for metrics, subscripts denote intercept (0), slopes (1) and study-treatment combination, *k*).

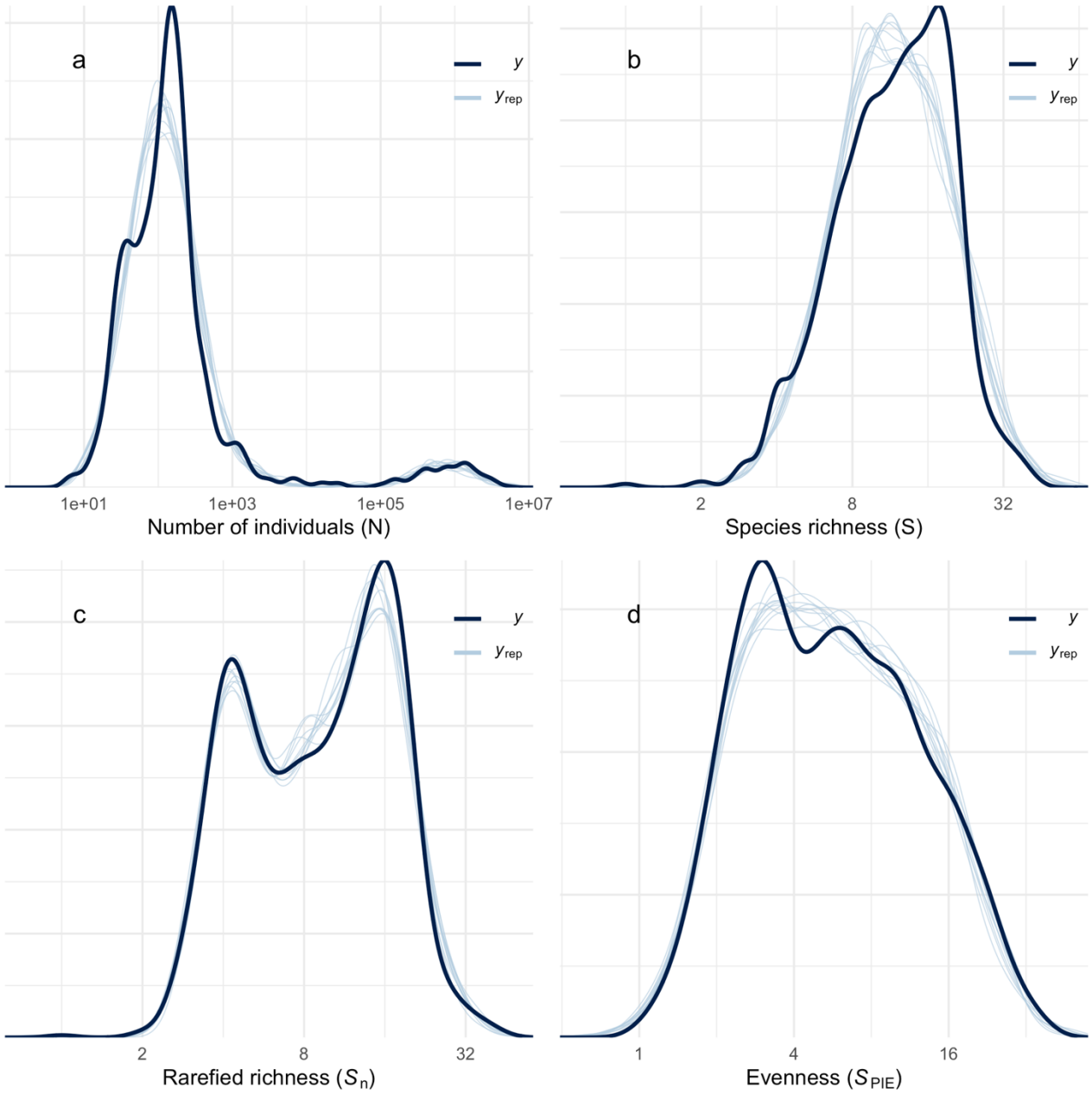

Figure S2: Posterior predictive checks for the model fit to the temporal data in perturbed environments. (a) Total numbers of individuals, (b) species richness, (c) rarefied richness (Sn) and (d) evenness (SPIE).). Each panel shows the density of the data (y) and ten draws of the posterior distribution (yrep).

References (for times series with experimental or natural perturbations)

Bateman, H., D. Childers, and P. Warren. 2018. Point-count bird censusing: long-term monitoring of bird abundance and diversity along the Salt River in the greater Phoenix metropolitan area, ongoing since 2013 ver 3.

Carpenter, S., J. Kitchell, J. Cole, and M. Pace. 2017. Cascade Project at North Temperate Lakes LTER Core Data Zooplankton 1984 - 2016 ver 4. Environmental Data Initiative.

Carpenter, S., J. Kitchell, J. Cole, and M. Pace. 2017. Cascade Project at North Temperate Lakes LTER Core Data Phytoplankton 1984 - 2015 ver 4. Environmental Data Initiative.

1012 Ellison, A. and R. Dunn. 2018. Ants Under Climate Change at Harvard Forest and Duke Forest
1013 2009-2015 ver 57. Environmental Data Initiative.
1014 Philip Grime and Jason Fridley. Point Quadrat Vegetation Data, Buxton Climate Change
1015 Experiment, UK, 1994-2009. Knowledge Network for Biocomplexity.
1016 doi:10.5063/AA/fridley.3.2.
1017 Hershey, A. 2016. Total numbers and species of insects taken from rock scrubbings during the
1018 summer of 1984-1988, 1993-1994, 1996-1998, in the Kuparuk River experimental reach near
1019 Toolik Field Station, North Slope Alaska.. ver 3. Environmental Data Initiative.
1020 Joern, A. 2020. CGR02 Sweep Sampling of Grasshoppers on Konza Prairie LTER watersheds
1021 ver 14. Environmental Data Initiative.
1022 Joern, A. 2020. PBG07 Grasshopper species abundances in the Patch-Burn Grazing experiment
1023 at Konza Prairie ver 5. Environmental Data Initiative.
1024 Knops, J. 2018. Arthropod sweep net sampling: Interactive Effects of Deer, Fire and Nitrogen
1025 ver 8. Environmental Data Initiative.
1026 Knops, J. 2018. Small mammal abundance: Interactive Effects of Deer, Fire and Nitrogen ver 8.
1027 Environmental Data Initiative.
1028 Santa Barbara Coastal LTER and D. Reed. 2020. SBC LTER: Reef: Long-term experiment: Kelp
1029 removal: Fish abundance ver 18. Environmental Data Initiative.
1030

1031

Spatial comparisons: natural environmental variation

We fit a model that assumed lognormal distributions for N, S_n, and S_{PIE}, and a Poisson distribution (and log link function) for S. We fit the model with four chains and 4000 iterations, with 2000 as warmup. The model took the following form:

$$N_{ij} \sim lognormal(\mu_{ij}^{N}, \sigma^{N}),$$

$$S_{ij} \sim poisson(\lambda_{ij}^{S}),$$

$$S_{n_{ij}} \sim lognormal(\mu_{ij}^{S_n}, \sigma^{S_n}),$$

$$S_{PIE_{ij}} \sim lognormal(\mu_{ij}^{S_{PIE}}, \sigma^{S_{PIE}}), \quad \text{(S1.4)}$$

$$\mu_{ij}^{N} = \beta_0^{N} + \beta_{0j}^{N} + (\beta_{1j}^{N}) site_{ij},$$

$$\log(\lambda_{ij}^{S}) = \beta_0^{S} + \beta_{0i}^{S} + \beta_{0j}^{S} + (\beta_{1j}^{S}) site_{ij},$$

$$\mu_{ij}^{S_n} = \beta_0^{S_n} + \beta_{0j}^{S_n} + (\beta_{1j}^{S_n}) site_{ij},$$

$$\mu_{ij}^{S_{PIE}} = \beta_0^{S_{PIE}} + \beta_{0j}^{S_{PIE}} + (\beta_{1j}^{S_{PIE}}) site_{ij},$$

$$\left[\beta_{0j}^{N}, \beta_{0j}^{S}, \beta_{0j}^{S_n}, \beta_{0j}^{S_{PIE}}, \beta_{1j}^{N}, \beta_{1j}^{S}, \beta_{1j}^{S_n}, \beta_{1j}^{S_{PIE}}\right]' \sim MVNormal(\mathbf{0}, \boldsymbol{SRS}),$$

$$\boldsymbol{S} = \begin{bmatrix} \sigma_{0j}^{N} & 0 & 0 & 0 & 0 & 0 & 0 & 0 \\ 0 & \sigma_{0j}^{S} & 0 & 0 & 0 & 0 & 0 & 0 \\ 0 & 0 & \sigma_{0j}^{S_n} & 0 & 0 & 0 & 0 & 0 \\ 0 & 0 & 0 & \sigma_{0j}^{S_{PIE}} & 0 & 0 & 0 & 0 \\ 0 & 0 & 0 & 0 & \sigma_{1j}^{N} & 0 & 0 & 0 \\ 0 & 0 & 0 & 0 & 0 & \sigma_{1j}^{S} & 0 & 0 \\ 0 & 0 & 0 & 0 & 0 & 0 & \sigma_{1j}^{S_n} & 0 \\ 0 & 0 & 0 & 0 & 0 & 0 & 0 & \sigma_{1j}^{S_{PIE}} \end{bmatrix},$$

$$\boldsymbol{R} = \begin{bmatrix} 1 & \rho_{N_{0j}S_{0j}} & \rho_{N_{0j}S_{n_{0j}}} & \rho_{N_{0j}S_{PIE_{0j}}} & \rho_{N_{0j}N_{1j}} & \rho_{N_{0j}S_{1j}} & \rho_{N_{0j}S_{n_{1j}}} & \rho_{N_{0j}S_{PIE_{1j}}} \\ \rho_{N_{0j}S_{0j}} & 1 & \rho_{S_{0j}S_{n_{0j}}} & \rho_{S_{0j}S_{PIE_{0j}}} & \rho_{S_{0j}N_{1j}} & \rho_{S_{0j}S_{1j}} & \rho_{S_{0j}S_{n_{1j}}} & \rho_{S_{0j}S_{PIE_{1j}}} \\ \rho_{N_{0j}S_{n_{0j}}} & \rho_{S_{0j}S_{n_{0j}}} & 1 & \rho_{S_{n_{0j}}S_{PIE_{0j}}} & \rho_{S_{n_{0j}}N_{1j}} & \rho_{S_{n_{0j}}S_{1j}} & \rho_{S_{n_{0j}}S_{n_{1j}}} & \rho_{S_{n_{0j}}S_{PIE_{1j}}} \\ \rho_{N_{0j}S_{PIE_{0j}}} & \rho_{S_{0j}S_{PIE_{0j}}} & \rho_{S_{n_{0j}}S_{PIE_{0j}}} & 1 & \rho_{S_{PIE_{0j}}N_{1j}} & \rho_{S_{PIE_{0j}}S_{1j}} & \rho_{S_{PIE_{0j}}S_{n_{1j}}} & \rho_{S_{PIE_{0j}}S_{PIE_{1j}}} \\ \rho_{N_{0j}N_{1j}} & \rho_{S_{0j}N_{1j}} & \rho_{S_{n_{0j}}N_{1j}} & \rho_{S_{PIE_{0j}}N_{1j}} & 1 & \rho_{N_{1j}S_{1j}} & \rho_{N_{1j}S_{n_{1j}}} & \rho_{N_{1j}S_{PIE_{1j}}} \\ \rho_{N_{0j}S_{1j}} & \rho_{S_{0j}S_{1j}} & \rho_{S_{n_{0j}}S_{1j}} & \rho_{S_{PIE_{0j}}S_{1j}} & \rho_{N_{1j}S_{1j}} & 1 & \rho_{S_{1j}S_{n_{1j}}} & \rho_{S_{1j}S_{PIE_{1j}}} \\ \rho_{N_{0j}S_{n_{1j}}} & \rho_{S_{0j}S_{n_{1j}}} & \rho_{S_{n_{0j}}S_{n_{1j}}} & \rho_{S_{PIE_{0j}}S_{n_{1j}}} & \rho_{N_{1j}S_{n_{1j}}} & \rho_{S_{1j}S_{n_{1j}}} & 1 & \rho_{S_{n_{1j}}S_{PIE_{1j}}} \\ \rho_{N_{0j}S_{PIE_{1j}}} & \rho_{S_{0k}S_{PIE_{1j}}} & \rho_{S_{n_{0j}}S_{PIE_{1j}}} & \rho_{S_{PIE_{0j}}S_{PIE_{1j}}} & \rho_{N_{1j}S_{PIE_{1j}}} & \rho_{S_{1j}S_{PIE_{1j}}} & \rho_{S_{n_{1j}}S_{PIE_{1j}}} & 1 \end{bmatrix},$$

$$\beta_0^{N}, \beta_0^{S}, \beta_0^{S_n}, \beta_0^{S_{PIE}} \sim N(0, 1),$$

$$\sigma^{N}, \sigma^{S_n}, \sigma^{S_{PIE}}, \sigma_{0i}^{S}, \sigma_{0j}^{N}, \sigma_{0j}^{S}, \sigma_{0j}^{S_n}, \sigma_{0j}^{S_{PIE}}, \sigma_{1j}^{N}, \sigma_{1j}^{S}, \sigma_{1j}^{S_n}, \sigma_{1j}^{S_{PIE}} \sim normal(0, 1),$$

$$\boldsymbol{R} \sim LJK(1),$$

where N_{ij}, S_{ij}, $S_{n_{ij}}$, and $S_{PIE_{ij}}$ are the values of each of the metrics for the ith observation in the jth study-site combination, and $site_{ij}$ is site identifier. β_0 (with the respective superscripts for each metric) represent the non-varying intercepts for each data source (one each for CESTES and

McGill), respectively. β_{0i}^{S} is an observation level varying intercept to model overdispersion in *S*. β_{0j} and β_{1j} (with the respective superscripts for each metric) represent the varying intercepts (reference sites for each study) and slopes (departures for all other sites). The covariance matrix of the multivariate normal distribution for varying study-site effects were parameterised in terms of a correlation matrix **R** and two matrices **S** with diagonal elements σ (superscripts for metrics, subscripts denote intercept (0), slopes (1)).

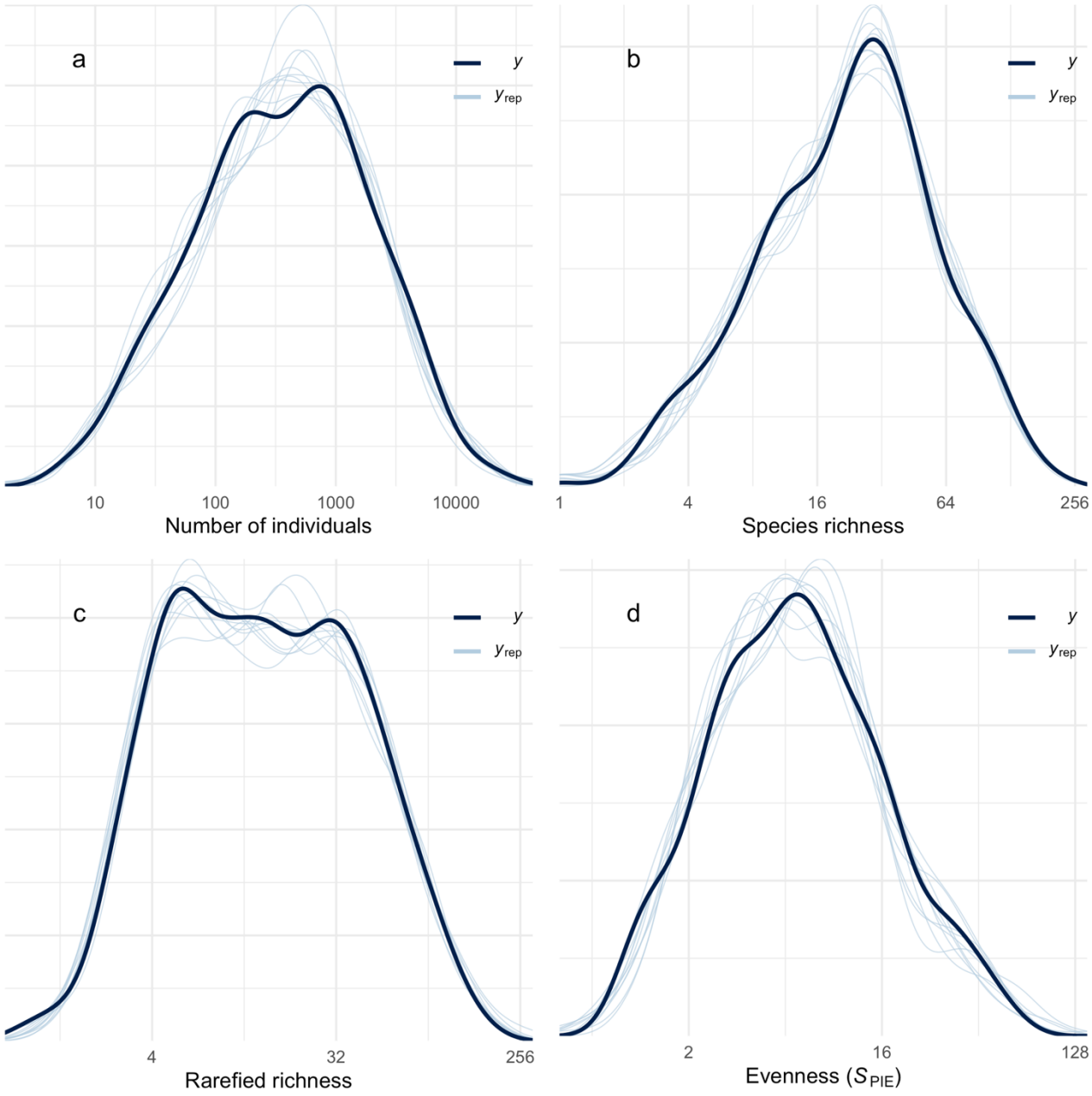

Figure S3: Posterior predictive checks for the model fit to the spatial data in natural environments. (a) Total numbers of individuals, (b) species richness, (c) rarefied richness (S_n) and (d) evenness (S_{PIE}). Each panel shows the density of the data (y) and ten draws of the posterior distribution (yrep).

Spatial comparisons: anthropogenic perturbations

We fit a model that assumed lognormal distributions for N, S_{n}, and S_{PIE}, and a Poisson distribution (and log link function) for S. We fit the model with four chains and 4000 iterations, with 2000 used as warmup. The model took the following form:

$$N_{ijk} \sim lognormal\left(\mu_{ijk}^{N}, \sigma^{N}\right),$$

$$S_{ijk} \sim poisson\left(\lambda_{ijk}^{S}\right),$$

$$S_{n_{ijk}} \sim lognormal\left(\mu_{ijk}^{S_n}, \sigma^{S_n}\right),$$

$$S_{PIE_{ijk}} \sim lognormal\left(\mu_{ijk}^{S_{PIE}}, \sigma^{S_{PIE}}\right),$$

$$\mu_{ijk}^{N} = \beta_0^{N} + \beta_{0j}^{N} + \beta_{0k}^{N} + (\beta_1^{N} + \beta_{1k}^{N}) LU_{ij},$$

$$\log\left(\lambda_{ijk}^{S}\right) = \beta_0^{S} + \beta_{0i}^{S} + \beta_{0j}^{S} + \beta_{0k}^{S} + (\beta_1^{S} + \beta_{1k}^{S}) LU_{ijk},$$

$$\mu_{ijk}^{S_n} = \beta_0^{S_n} + \beta_{0j}^{S_n} + \beta_{0k}^{S_n} + (\beta_1^{S_n} + \beta_{1k}^{S_n}) LU_{ijk},$$

$$\mu_{ijk}^{S_{PIE}} = \beta_0^{S_{PIE}} + \beta_{0j}^{S_{PIE}} + \beta_{0k}^{S_{PIE}} + (\beta_1^{S_{PIE}} + \beta_{1k}^{S_{PIE}}) LU_{ijk},$$

$$\left[\beta_{0j}^{N}, \beta_{0j}^{S}, \beta_{0j}^{S_n}, \beta_{0j}^{S_{PIE}}, \beta_{1j}^{N}, \beta_{1j}^{S}, \beta_{1j}^{S_n}, \beta_{1j}^{S_{PIE}}\right]' \sim MVNormal(\mathbf{0}, \boldsymbol{SRS}),$$

$$\boldsymbol{S} = \begin{bmatrix} \sigma_{0k}^{N} & 0 & 0 & 0 & 0 & 0 & 0 & 0 \\ 0 & \sigma_{0k}^{S} & 0 & 0 & 0 & 0 & 0 & 0 \\ 0 & 0 & \sigma_{0k}^{S_n} & 0 & 0 & 0 & 0 & 0 \\ 0 & 0 & 0 & \sigma_{0k}^{S_{PIE}} & 0 & 0 & 0 & 0 \\ 0 & 0 & 0 & 0 & \sigma_{1k}^{N} & 0 & 0 & 0 \\ 0 & 0 & 0 & 0 & 0 & \sigma_{1k}^{S} & 0 & 0 \\ 0 & 0 & 0 & 0 & 0 & 0 & \sigma_{1k}^{S_n} & 0 \\ 0 & 0 & 0 & 0 & 0 & 0 & 0 & \sigma_{1k}^{S_{PIE}} \end{bmatrix},$$

$$\boldsymbol{R} = \begin{bmatrix} 1 & \rho_{N_{0k}S_{0k}} & \rho_{N_{0k}S_{n0k}} & \rho_{N_{0k}S_{PIE0k}} & \rho_{N_{0k}N_{1k}} & \rho_{N_{0k}S_{1k}} & \rho_{N_{0k}S_{n1k}} & \rho_{N_{0k}S_{PIE1k}} \\ \rho_{N_{0k}S_{0k}} & 1 & \rho_{S_{0k}S_{n0k}} & \rho_{S_{0k}S_{PIE0k}} & \rho_{S_{0k}N_{1k}} & \rho_{S_{0k}S_{1k}} & \rho_{S_{0k}S_{n1k}} & \rho_{S_{0k}S_{PIE1k}} \\ \rho_{N_{0k}S_{n0k}} & \rho_{S_{0k}S_{n0k}} & 1 & \rho_{S_{n0k}S_{PIE0k}} & \rho_{S_{n0k}N_{1k}} & \rho_{S_{n0k}S_{1k}} & \rho_{S_{n0k}S_{n1k}} & \rho_{S_{n0k}S_{PIE1k}} \\ \rho_{N_{0k}S_{PIE0k}} & \rho_{S_{0k}S_{PIE0k}} & \rho_{S_{n0k}S_{PIE0k}} & 1 & \rho_{S_{PIE0k}N_{1k}} & \rho_{S_{PIE0k}S_{1k}} & \rho_{S_{PIE0k}S_{n1k}} & \rho_{S_{PIE0k}S_{PIE1k}} \\ \rho_{N_{0k}N_{1k}} & \rho_{S_{0k}N_{1k}} & \rho_{S_{n0k}N_{1k}} & \rho_{S_{PIE0k}N_{1k}} & 1 & \rho_{N_{1k}S_{1k}} & \rho_{N_{1k}S_{n1k}} & \rho_{N_{1k}S_{PIE1k}} \\ \rho_{N_{0k}S_{1k}} & \rho_{S_{0k}S_{1k}} & \rho_{S_{n0k}S_{1k}} & \rho_{S_{PIE0k}S_{1k}} & \rho_{N_{1k}S_{1k}} & 1 & \rho_{S_{1k}S_{n1k}} & \rho_{S_{1k}S_{PIE1k}} \\ \rho_{N_{0k}S_{n1k}} & \rho_{S_{0k}S_{n1k}} & \rho_{S_{n0k}S_{n1k}} & \rho_{S_{PIE0k}S_{n1k}} & \rho_{N_{1k}S_{n1k}} & \rho_{S_{1k}S_{n1k}} & 1 & \rho_{S_{n1k}S_{PIE1k}} \\ \rho_{N_{0k}S_{PIE1k}} & \rho_{S_{0k}S_{PIE1k}} & \rho_{S_{n0k}S_{PIE1i}} & \rho_{S_{PIE0k}S_{PIE1k}} & \rho_{N_{1k}S_{PIE1k}} & \rho_{S_{1k}S_{PIE1k}} & \rho_{S_{n1k}S_{PIE1k}} & 1 \end{bmatrix},$$

$$\beta_0^{N}, \beta_1^{N} \sim student(3, 5, 10),$$

$$\beta_0^{S}, \beta_1^{S} \sim student(3, 3, 10),$$

$$\beta_0^{S_n}, \beta_0^{S_{PIE}}, \beta_1^{S_n}, \beta_1^{S_{PIE}} \sim student(3, 2, 10),$$

$$\sigma^{N}, \sigma^{S_n}, \sigma^{S_{PIE}}, \sigma_{0i}^{S}, \sigma_{0j}^{N}, \sigma_{0j}^{S}, \sigma_{0j}^{S_n}, \sigma_{0j}^{S_{PIE}}, \sigma_{0k}^{N}, \sigma_{0k}^{S}, \sigma_{0k}^{S_n}, \sigma_{0k}^{S_{PIE}}, \sigma_{1k}^{N}, \sigma_{1k}^{S}, \sigma_{1k}^{S_n}, \sigma_{1k}^{S_{PIE}} \sim student(3, 0, 10),$$

$$\boldsymbol{R} \sim LJK(1),$$

where N_{ijk}, S_{ijk}, $S_{n_{ijk}}$, and $S_{PIE_{ijk}}$ are the values of each of the metrics for the *i*th concatenation of source ID, study number, block and site number (denoted SSBS in the database), in the *j*th concatenation of source ID, study number, block (denoted SSB in the database), of the *k*th combination of source ID and study (denoted SS in the database), and LU is an identifier for land use types (other than primary vegetation, that was fit as the intercept). β_0 (with the respective superscripts for each metric) represent the non-varying intercepts for reference land use category (i.e., primary vegetation). β_{0i}^{S} is a site-level varying intercept to model overdispersion in *S*. β_{0j} (with the respective superscripts for each metric) is a varying intercept for blocks. β_{0k} and β_{1k} (with the respective superscripts for each metric) represent the varying intercepts (reference sites for each study) and slopes (departures for all other sites). The covariance matrix of the multivariate normal distribution for varying study-site effects were parameterised in terms of a correlation matrix **R** and two matrices **S** with diagonal elements σ (superscripts for metrics, subscripts denote intercept (0), slopes (1)).

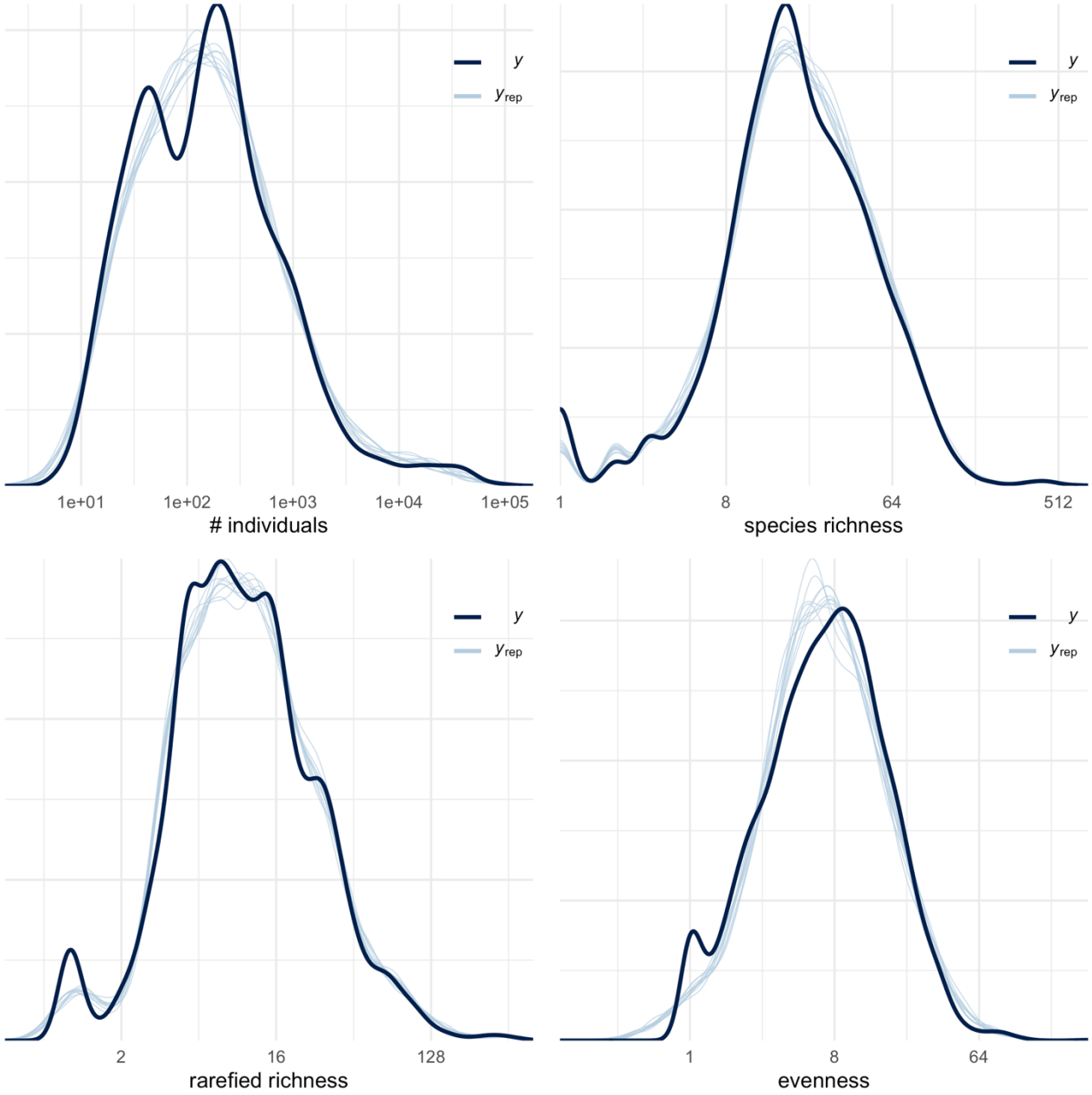

Figure S4: Posterior predictive checks for the model fit to the spatial data in anthropogenically perturbed environments. (a) Total numbers of individuals, (b) species richness, (c) rarefied richness (S_n) and (d) evenness (S_{PIE}). Each panel shows the density of the data (y) and ten draws of the posterior distribution (yrep).

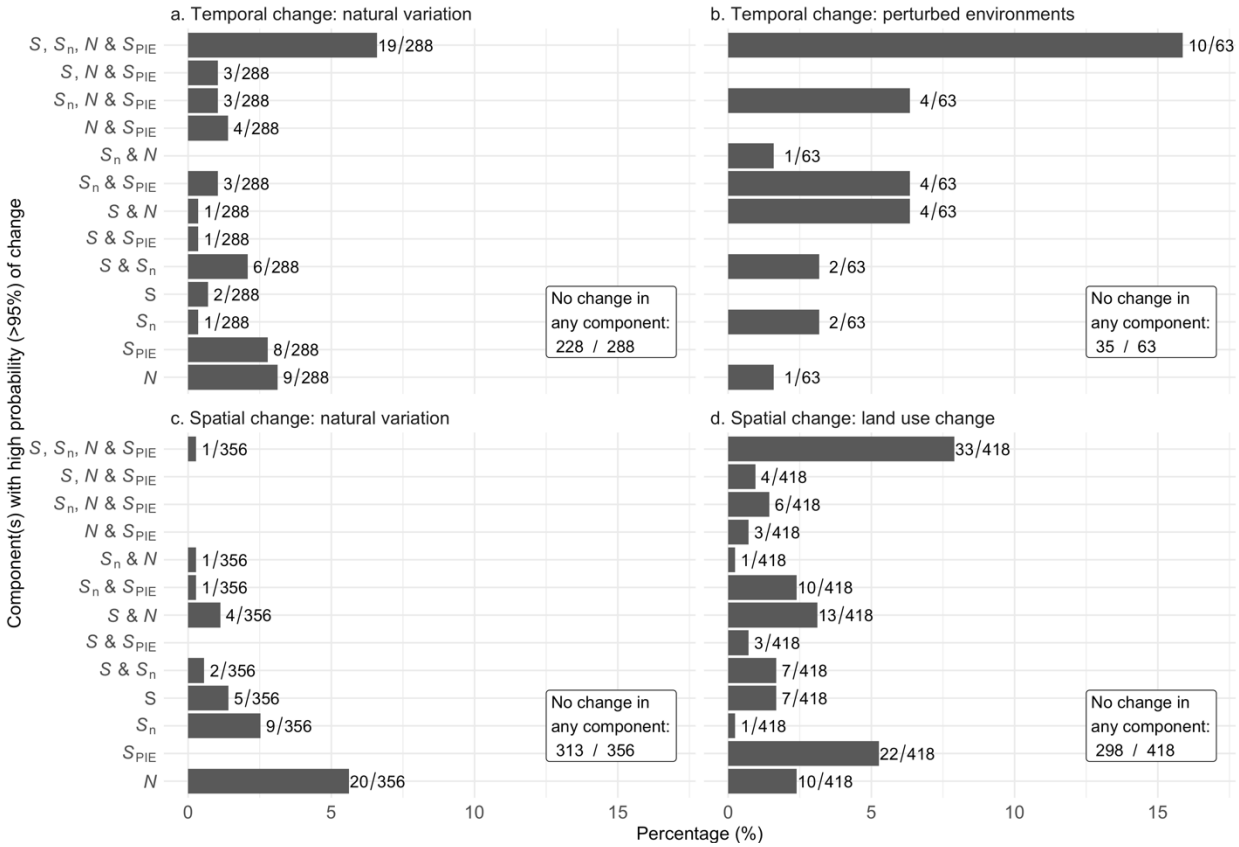

Figure S5: Summary of assemblage diversity components with a high probability of change (90% credible interval did not overlap zero).(a) temporal changes in naturally varying environments, (b) temporal changes in perturbed environments, (c) spatial changes relative to an arbitrary reference, (d) spatial changes relative to primary vegetation. Assemblages with no component changes different from zero are reported as insets for clarity. Metric abbreviations: total number of individuals (N), expected number of species for n individuals (S_n), numbers equivalent transformation of the Probability of Interspecific Encounter (S_{PIE}), and total species richness (S). Number following each bar is the count of assemblages for that category.

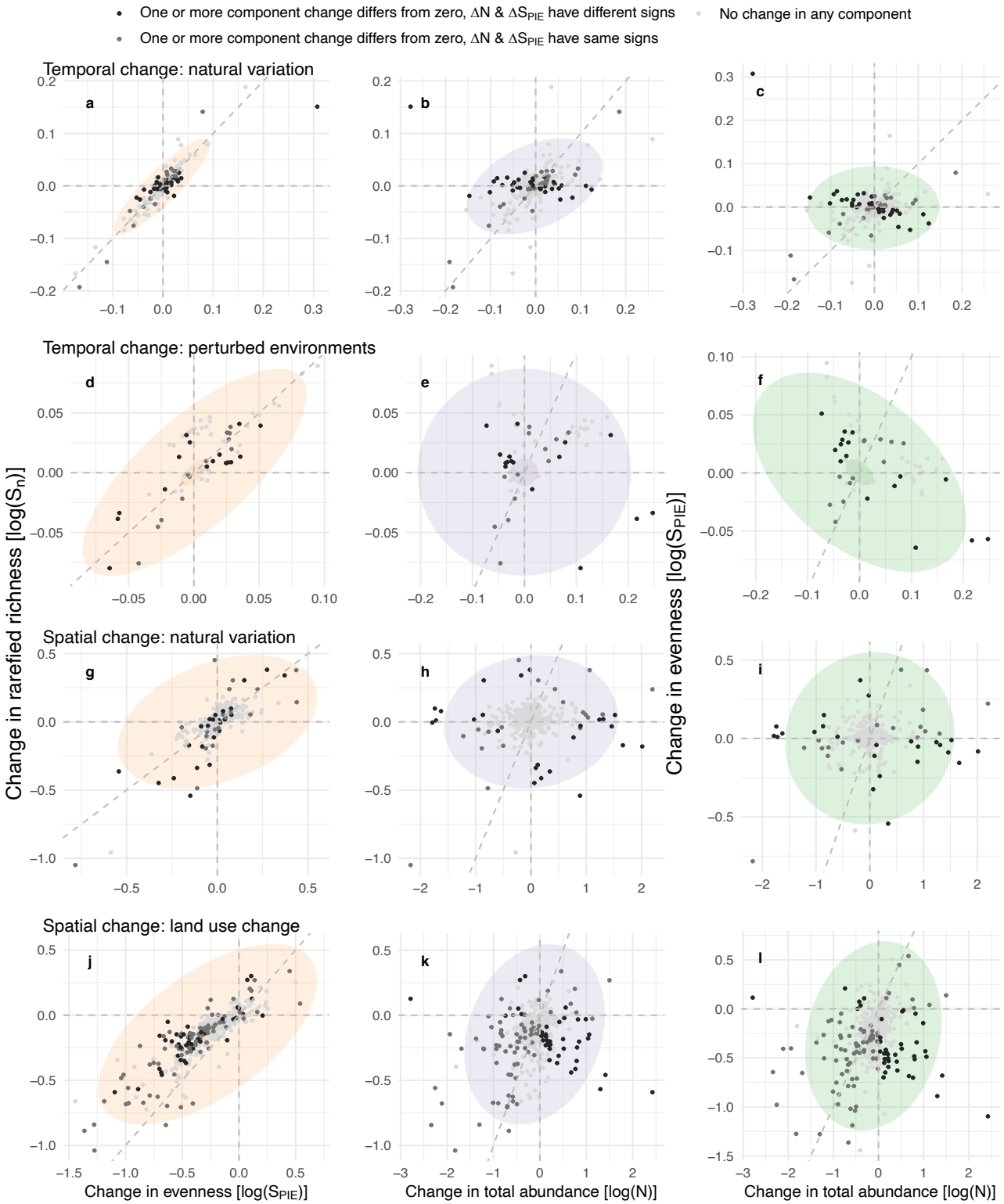

Figure S6: Relationships between four components of local diversity change (not shown on Figure 3). Change in rarefied richness as a function of changes in evenness (left), change in rarefied richness as a function of changes in total abundance (middle) and evenness (right) for (a-c) study-level estimates of temporal changes in naturally varying environments; (d-f) estimates of temporal change for combinations of study and treatment in perturbed environments; (c) estimates of spatial changes within studies from an arbitrary reference site along natural

environmental gradients; and, (d) estimates of spatial change within studies between primary vegetation and different land use categories. Coloured concentration ellipses show 10% increments (5 – 95%) of the posterior distributions. Dotted grey lines are x = y = 0, and x = y for visual reference. NB: Scale of x- and y-axes vary between data sources; one estimate with $\Delta N = -1.79$, $\Delta S = -3.77$, $\Delta Sn = -3.23$, $\Delta SPIE = -3.21$, removed from (j-l) for clarity.